NACA RM E53J08

NACA

RESEARCH MEMORANDUM

CORRELATION OF ISOTHERMAL CONTOURS FORMED BY PENETRATION OF JET OF LIQUID AMMONIA DIRECTED NORMAL TO AN AIR STREAM

By David B. Fenn

Lewis Flight Propulsion Laboratory
Cleveland, Ohio

NATIONAL ADVISORY COMMITTEE
FOR AERONAUTICS

WASHINGTON
February 3, 1954

NATIONAL ADVISORY COMMITTEE FOR AERONAUTICS

RESEARCH MEMORANDUM

CORRELATION OF ISOTHERMAL CONTOURS FORMED BY PENETRATION OF JET OF LIQUID AMMONIA DIRECTED NORMAL TO AN AIR STREAM

By David B. Fenn

SUMMARY

An investigation was conducted to correlate the isothermal contour lines formed downstream of a single jet of liquid ammonia directed normal to an air stream. Criteria are presented to facilitate the design of jet-engine thrust-augmentation systems utilizing the injection of liquid ammonia to cool the air at the compressor inlet. From the correlation presented, it is possible to construct an isothermal contour map for a single orifice operating within the following range of conditions: air velocity, 112 to 329 feet per second; air density, 0.024 to 0.070 pound per cubic foot; air temperature, 534° to 770° R; ammonia jet velocity, 63 to 244 feet per second; ammonia temperature, 433° to 470° R; mixing distance, 4 to 24 inches; orifice diameter, 0.018 to 0.053 inch. It was verified that the construction of the isothermal contours formed by a multiorifice injection system may be determined by simply adding the temperature drops of the overlapping single-orifice contour maps determined from the correlation.

INTRODUCTION

One method of augmenting the thrust of a turbojet engine is to cool the air entering or passing through the compressor. Water-alcohol mixtures have been extensively used as coolants because of their high latent heat of vaporization. The high boiling point of the water-alcohol mixtures, however, restricts their application to flight conditions for which the inlet-air temperature is relatively high, principally take-off. For low inlet-air temperatures, such as those encountered during high-altitude flight in the transonic speed range, liquid ammonia is an attractive coolant because of its low boiling point even though its latent heat of vaporization is only about one-half that of water. However, liquid ammonia would not be an effective coolant at low altitudes (ref. 1) where the atmosphere is relatively moist, because it combines exothermically with water to form ammonium hydroxide.

One of the basic requirements of an inlet coolant-injection system is that it distribute the coolant as evenly as possible in the inlet-air stream in order to provide a uniform temperature at the compressor inlet. It is evident that the penetration and cooling characteristics of the injected liquid must be known before an adequate injection system can be designed. In order to provide the needed information, an investigation was conducted at the NACA Lewis laboratory to measure and to correlate the isothermal contours formed by the penetration of a single jet of liquid ammonia directed normal to an air stream.

Data for this investigation were obtained at several distances downstream of the point of injection for several orifice diameters over ranges of ammonia-to-air velocity, density, and temperature ratios. A correlation of the temperature profile in a plane containing the axis of the ammonia jet is presented, together with a correlation of the maximum width of the isothermal contour map formed by the penetration of the jet of liquid ammonia into the air stream. The method of correlation employed in this investigation is similar to that used in references 2 and 3 to correlate the penetration characteristics of water and heated-air jets directed normal to an air stream.

From the correlations presented herein, it is possible (within the range of variables considered) to construct an isothermal contour map for a particular design application and to predict the temperature gradients formed by the injection system. In order to demonstrate a simple method of extending the single-orifice correlation to a multi-orifice injection system, a prediction of the isothermal contour map formed by a double-orifice system is made and compared with experimental results.

APPARATUS

Air System

The apparatus for this investigation was installed in a 21-inch-diameter duct which was connected to the laboratory dry-air system as schematically indicated in figure 1. Four combustor-type preheaters were used to obtain air temperatures from 80° to 300° F, and the desired stream velocity and density were established in the duct by regulating the air flow through the inlet and exhaust control valves. The quantity of air flowing through the system was measured by a calibrated A.S.M.E. type orifice located upstream of the inlet-air control valves.

Ammonia System

Liquid anhydrous ammonia was supplied at various temperatures and pressures to a single-orifice spray bar which injected the ammonia normal to the air flow in the 21-inch-diameter duct. In order to maintain the ammonia in its liquid state, the system was pressurized with helium from tanks connected to the ammonia storage tank (fig. 2). Liquid ammonia from the storage tank was passed through rotameters and a filter to the heat exchanger where it was cooled by the evaporation of ammonia surrounding the heat-exchanger coils. The temperature of the measured ammonia flow was controlled by varying the pressure and, hence, the evaporation rate of the surrounding ammonia in the heat exchanger. The pressurized ammonia from the heat exchanger was passed through the throttle to the spray bar shown in figure 3. In order to prevent heating of the ammonia as it flowed from the heat exchanger to the spray orifice, the connecting lines were insulated. The temperature of the liquid ammonia was measured by means of a thermocouple installed within the spray bar close to the orifice. The three single-orifice spray bars investigated had orifice diameters of 0.018, 0.029, and 0.053 inch. In addition, a two-orifice spray bar was used which was similar to the single-orifice bars except that it had two 0.031-inch-diameter orifices 1 inch apart.

Test Section

The spray bar was located 5 inches from the bottom of the duct with the orifice directed upward on the vertical center line of the duct. In order to determine the isothermal contour lines formed by the ammonia jet, a twin-armed swinging rake equipped with aspirating thermocouples was installed in the duct (fig. 4). The thermocouple probes were pointed downstream to prevent droplets of liquid ammonia from contacting the thermocouple junctions, and the rake body was connected to the laboratory exhaust system to provide a continuous flow of gas through the thermocouple probes. A detailed sketch of the aspirating thermocouple probes is shown in figure 5. The mixing distance between the spray bar and the swinging survey rake was varied by altering the axial location of the spray bar in the duct.

Other instrumentation in the test section provided for the measurement of duct static pressure by means of three wall static taps 30 inches upstream of the survey rake (fig. 4) and the measurement of total air temperature with an 8-inch immersion thermocouple in the 8-foot straight section upstream of the survey rake.

CORRELATION PROCEDURE

Characteristics of Isothermal Contour Maps

From the temperature surveys made with the swinging rake described in the previous section, maps of constant temperature drop were constructed to define the penetration and cooling characteristics of the jet of liquid ammonia. Samples of these isothermal contour maps are presented in figure 6 for a range of air velocities. The slight displacement of all the contour maps from the vertical center line of the duct is attributed to some residual whirl of the air in the duct. It is believed that the experimental results obtained during this investigation were unaffected by the slight displacement of the isothermal maps.

In order to achieve a correlation of these isothermal contours, it was necessary to establish a method of defining the map in terms of its geometric dimensions. Accordingly, the maps were considered to be symmetrical about an axis containing both the maximum depth of penetration and the maximum temperature drop. It was decided that the isothermal contour map could be approximated if two temperature profiles, one along the axis of symmetry and one through the center of the map perpendicular to the axis of symmetry, were known. The axes of these temperature profiles are shown as dashed lines in figure 6.

A sketch of an isothermal contour map together with the temperature profiles existing along and perpendicular to the axis of symmetry is presented in figure 7. (The symbols used in figure 7 and elsewhere in this report are defined in appendix A.) The temperature profile along the axis of symmetry can be closely approximated by three straight lines as illustrated by figure 8, where typical temperature profiles are presented for a range of air velocities. The agreement between the tangents and the actual temperature profile along the axis of symmetry was particularly good on the upper portion of the profile. The center line of tne spray bar was chosen as the datum line of this temperature profile, and the dimensions which will be correlated to define it are: y_1, y_2, y_3, y_4, and ΔT_m (fig. 7).

The temperature profile in a direction perpendicular to the axis of symmetry was obtained by cross-plotting from the isothermal contour map. These cross plots revealed that this temperature profile could be closely approximated by assuming a linear variation of temperature between the isotherm for a temperature drop of 5° F and that for maximum temperature drop ΔT_m. It was further observed that the isotherm of maximum temperature drop ΔT_m could be considered to be circular ($x_2 = y_3 - y_4$ in fig. 7). Therefore, the only dimension required to complete the correlation of the isothermal contour map is the distance between lines of 5° F temperature drop (x_1).

Derivation of Correlation Equation

The dimensional analysis and experimental results of references 2 and 3 indicate that an equation of the form

$$\frac{y}{\sqrt{C}\,D_j} = K\left(\frac{V_j}{V_O}\right)^a\left(\frac{\rho_j}{\rho_O}\right)^b\left(\frac{S}{\sqrt{C}\,D_j}\right)^c \tag{1}$$

may be used to correlate the penetration characteristics of water and heated air jets directed normal to an air stream. The injection of liquid ammonia into an air stream, however, introduces an added complication in that the ammonia changes rapidly from the liquid to the gaseous state after injection. The evaporation rate of the liquid is dependent upon its vapor pressure and the conditions of pressure and temperature existing in the air stream. Because the vapor pressure of the liquid is a function of the liquid temperature T_j, and because the air temperature can be varied independently of the air density, an additional dimensionless ratio T_j/T_O was added to equation (1). The resulting correlation equation was then written as follows:

$$\frac{y}{\sqrt{C}\,D_j} = K\left(\frac{V_j}{V_O}\right)^a\left(\frac{\rho_j}{\rho_O}\right)^b\left(\frac{T_j}{T_O}\right)^c\left(\frac{S}{\sqrt{C}\,D_j}\right)^d \tag{2}$$

Equation (2) was used to correlate the linear dimensions (y_1, y_2, y_3, y_4, and x_1) of the temperature profiles along and perpendicular to the axis of symmetry of the contour map (fig. 7). In order to correlate the maximum temperature drop ΔT_m occurring at the center of the contour map, the correlation equation was written in the following form:

$$\frac{\Delta T_m}{T_O - T_j} = K_t\left(\frac{V_j}{V_O}\right)^e\left(\frac{\rho_j}{\rho_O}\right)^f\left(\frac{T_j}{T_O}\right)^g\left(\frac{S}{\sqrt{C}\,D_j}\right)^h \tag{3}$$

The general procedure followed in obtaining the data for this investigation was to hold three of the terms on the right side of the correlation equation constant and to determine the variation of the remaining term with the quantity being correlated. In this manner, the exponent of each term in the general correlation equation was evaluated for each of the dimensions correlated. The data obtained in this investigation are presented in table I and include the following range of variables:

Variable	Range
Air velocity, ft/sec	112-329
Air density, lb/cu ft	0.024-0.070
Air temperature, $^{\circ}R$	534-770
Ammonia jet velocity, ft/sec	63-244
Ammonia temperature, $^{\circ}R$	433-470
Mixing distance, in.	4-24
Orifice diameter, in.	0.018-0.053

The methods of calculation used in this investigation are presented in appendix B.

EVALUATION OF EXPONENTS AND CONSTANTS

Correlation of Temperature Profile Along Axis of Symmetry

Boundary dimension y_1. - The distance between the spray-bar center line and the intersection of the upper bounding tangent of the temperature profile along the axis of symmetry of the isothermal contour map with the line of zero temperature drop was defined as y_1 (fig. 7).

The correlation equation for the bounding dimension y_1 was written as follows:

$$\frac{y_1}{\sqrt{C}\ D_j} = K_1 \left(\frac{V_j}{V_O}\right)^a \left(\frac{\rho_j}{\rho_O}\right)^b \left(\frac{T_j}{T_O}\right)^c \left(\frac{S}{\sqrt{C}\ D_j}\right)^d \tag{4}$$

The exponent of the velocity ratio V_j/V_O was determined by holding the remaining terms of equation (4) constant and plotting the variation of the penetration parameter $y_1/\sqrt{C}\ D_j$ with the velocity ratio on logarithmic coordinates as shown in figure 9(a). Data are shown for two density ratios, each set of which may be represented by a straight line having a slope of 0.77. The exponent of the velocity ratio is therefore 0.77. The exponent of the density ratio ρ_j/ρ_O was determined in a similar manner for two temperature ratios, and an exponent of 0.53 was obtained (fig. 9(b)). The effect of the temperature ratio on the penetration parameter $y_1/\sqrt{C}\ D_j$ is illustrated in figure 9(c) for two density ratios. In order to maintain the ammonia in its liquid state in the spray bar, the temperature of the ammonia was restricted in this investigation to a range of from 433° to 470° R. Although the range of T_j is not large, it covers all cases of practical interest. The exponent of the temperature ratio was found to be 1.1 (fig. 9(c)).

The effect of the ratio of mixing distance to effective diameter was obtained by plotting the quantity $(y_1/\sqrt{C}\ D_j)/(V_j/V_0)^{0.77}\ (\rho_j/\rho_0)^{0.53}\ (T_j/T_0)^{1.1}$ as a function of $S/\sqrt{C}\ D_j$ on figure 9(d). These data include three mixing distances and three orifice diameters and may be approximately represented by a line with a slope of 0.72.

The remaining unknown required to complete the correlation of the penetration parameter $y_1/\sqrt{C}\ D_j$ is the coefficient K_1. In evaluating this coefficient, the penetration parameter was plotted as a function of the quantity $(V_j/V_0)^{0.77}\ (\rho_j/\rho_0)^{0.53}\ (T_j/T_0)^{1.1}\ (S/\sqrt{C}\ D_j)^{0.72}$ (fig. 9(e)). Substitution of coordinate values into the correlation equation yielded a value of K_1 equal to 0.214. The working equation for the boundary dimension y_1 is then

$$\frac{y_1}{\sqrt{C}\ D_j} = 0.214 \left(\frac{V_j}{V_0}\right)^{0.77} \left(\frac{\rho_j}{\rho_0}\right)^{0.53} \left(\frac{T_j}{T_0}\right)^{1.1} \left(\frac{S}{\sqrt{C}\ D_j}\right)^{0.72} \tag{5}$$

Boundary dimension y_2. - The distance between the spray-bar center line and the intersection of the lower-boundary tangent of the temperature profile along the axis of symmetry with a line of zero temperature drop was defined as y_2 (fig. 7). However, because the dimension y_2 becomes negative under certain conditions, the quantity $(y_1 - y_2)/\sqrt{C}\ D_j$ was chosen as the lower-boundary defining parameter. By a process similar to that used to correlate the penetration parameter $y_1/\sqrt{C}\ D_j$, the following equation was developed:

$$\frac{y_1 - y_2}{\sqrt{C}\ D_j} = K_2 \left(\frac{V_j}{V_0}\right)^{0.60} \left(\frac{\rho_j}{\rho_0}\right)^{0.45} \left(\frac{T_j}{T_0}\right)^{1.1} \left(\frac{S}{\sqrt{C}\ D_j}\right)^{0.72} \tag{6}$$

The lower-boundary parameter $(y_1 - y_2)/\sqrt{C}\ D_j$ is presented as a function of the right side of equation (6) in figure 10. Substitution of coordinate values from figure 10 into equation (6) yields a value of K_2 equal to 0.317, and equation (6) becomes

$$\frac{y_1 - y_2}{\sqrt{C}\ D_j} = 0.317 \left(\frac{V_j}{V_0}\right)^{0.6} \left(\frac{\rho_j}{\rho_0}\right)^{0.45} \left(\frac{T_j}{T_0}\right)^{1.1} \left(\frac{S}{\sqrt{C}\ D_j}\right)^{0.72} \tag{7}$$

Maximum temperature drop ΔT_m. - The maximum temperature drop occurring at the center of the isothermal contour map must be known before a temperature profile along the axis of symmetry (fig. 7) can be constructed. The dimensionless parameter selected for this correlation was $\Delta T_m/(T_0 - T_j)$, and by a process similar to that previously described the following correlation equation was developed:

$$\frac{\Delta T_m}{T_0 - T_j} = K_t \left(\frac{V_j}{V_0}\right)^{0.6} \left(\frac{\rho_j}{\rho_0}\right)^{1.0} \left(\frac{T_j}{T_0}\right)^{4.0} \left(\frac{S}{\sqrt{C}\, D_j}\right)^{-0.9} \tag{8}$$

The maximum-temperature-drop parameter $\Delta T_m/(T_0 - T_j)$ is presented as a function of the right side of equation (8) in figure 11 to determine the value of K_t. The value of K_t as determined from figure 11 is 0.838, and equation (8) may be written as

$$\frac{\Delta T_m}{T_0 - T_j} = 0.838 \left(\frac{V_j}{V_0}\right)^{0.6} \left(\frac{\rho_j}{\rho_0}\right)^{1.0} \left(\frac{T_j}{T_0}\right)^{4.0} \left(\frac{S}{\sqrt{C}\, D_j}\right)^{-0.9} \tag{9}$$

Boundary dimensions y_3 and y_4. - The distances between the spray-bar center line and the intersections of the upper and lower tangents of the temperature profile along the axis of symmetry with the tangent to the point of maximum temperature drop were defined as y_3 and y_4, respectively (fig. 7). It was found that y_3 and y_4 could be correlated with y_1 as illustrated in figure 12. Although these correlations are not rigorous, they afford a simple determination of these dimensions when y_1 has been found from the general equation.

Correlation of Temperature Profile Perpendicular to Axis of Symmetry

The temperature profile along a line through the center of the isothermal contour map perpendicular to the axis of symmetry may be approximated if the dimensions x_1, x_2, and ΔT_m are known (fig. 7). A correlation of the maximum temperature drop ΔT_m is presented in the previous section. The dimension x_2 can be assumed to be equal to $y_3 - y_4$ as discussed in the section CORRELATION PROCEDURE. The distance x_1 perpendicular to the axis of symmetry between lines of 5° F temperature drop is therefore the only additional dimension required to complete the correlation of this temperature profile. The

isothermal contour maps possess a similarity of shape which permitted a correlation of the maximum horizontal width parameter x_1/D_j as a function of the previously correlated parameter $(y_1 - y_2)/D_j$. This correlation, which is presented in figure 13, affords a simple approach to the solution of design problems.

APPLICATION OF CORRELATION

The correlation presented provides a means of predicting the isothermal contour map formed by a single jet of liquid ammonia directed normal to an air stream. In order to design a multiorifice injection system from this correlation, two assumptions can be made: (1) The temperature drop at any point within the ammonia spray field is proportional to the quantity of ammonia present, and (2) the effects of droplet impingement are negligible. Naturally, the assumption that the temperature drop is proportional to the quantity of ammonia present fails when the air becomes saturated with ammonia. Figure 14 shows the limiting temperature drop obtainable by saturating dry air with ammonia; the temperature drops indicated cannot be exceeded.

To substantiate the two assumptions, data were obtained from a double-orifice spray bar, and a prediction of the resulting isothermal contour map is made from the single-orifice correlation. For the conditions under which the two-orifice data were obtained, temperature profiles along and perpendicular to the axis of symmetry for a single orifice were constructed from the correlation and are presented in figures 15(a) and (b). An isothermal contour map for the single orifice was then constructed by fairing the isotherms between points of known temperature along and perpendicular to the axis of symmetry. The two such single-orifice contour maps presented in figure 15(c) are displaced from each other by a distance equal to the spacing of the orifices on the double-orifice spray bar. The contour map for the double-orifice system was then constructed by adding the temperature drops of the overlapping single-orifice maps. As an aid to the combining of the overlapping maps, a composite temperature profile perpendicular to the axis of symmetry was constructed (fig. 15(d)) by adding the temperature drops (ΔT) of two single-orifice temperature profiles displaced from each other by the distance between orifices. The isothermal contour map predicted in this manner for the double-orifice injection system is represented in figure 15(e) by solid lines, which are in good agreement with the experimentally measured contour map represented by dashed lines. To compensate for the slight whirl present in the duct, the experimental contour map was rotated so that its axis would coincide with that of the predicted contour map. It is believed that with the assumptions made to predict the isothermal contours formed by a multiorifice injection system sufficiently accurate results for most engineering designs can be obtained.

CONCLUDING REMARKS

An empirical correlation was developed by means of which the isothermal contour lines formed downstream of a single jet of liquid ammonia directed normal to an air stream can be predicted. From this correlation, the isothermal contour lines formed by a multiplicity of ammonia jets can be approximated with sufficient accuracy for most engineering applications.

Lewis Flight Propulsion Laboratory
National Advisory Committee for Aeronautics
Cleveland, Ohio, November 9, 1953

APPENDIX A

SYMBOLS

The following symbols are used in this report:

A	area, sq ft
C	coefficient of discharge
D	diameter, in.
g	acceleration due to gravity, 32.16 ft/sec^2
K	coefficient
p	static pressure, lb/sq ft abs
R	gas constant for air, 53.4 ft-lb/(lb)($^\circ$R)
S	mixing distance between spray bar and swinging survey rake, in.
T	indicated temperature, $^\circ$R
ΔT	difference between air-stream temperature and temperature at some point within the ammonia spray field, $^\circ$F
V	velocity, ft/sec
w	weight flow, lb/sec
x	dimension normal to axis of symmetry of isothermal contour map, in.
y	dimension along axis of symmetry of isothermal contour map, in.
ρ	density, lb/cu ft
a,b,c,d e,f,g	exponents

Subscripts:

i	ideal conditions
j	conditions in ammonia jet
m	maximum condition
t	temperature correlation
0	conditions in air stream
1,2,3,4	linear correlations (see fig. 7)

APPENDIX B

METHODS OF CALCULATION

Air density was calculated from the equation of state:

$$\rho_O = \frac{p_O}{R_O T_O} \text{ lb/cu ft}$$

where the value of R_O was taken as 53.4 ft-lb/(lb)($^\circ$R).

The velocity of the air stream V_O was computed from the air density ρ_O and the measured air flow by the continuity equation

$$V_O = \frac{w_O}{\rho_O A_O} \text{ ft/sec}$$

Properties of liquid ammonia were obtained from reference 4 and the jet velocity was calculated from Bernoulli's equation

$$V_j = \sqrt{2g \frac{p_j - p_O}{\rho_j}}$$

where V_j is the ideal velocity of a liquid jet issuing from an orifice.

The coefficient of discharge of the orifices was defined as the ratio of the measured to the ideal ammonia flow. Ideal ammonia flow was calculated from the following equation:

$$w_i = \rho_j A_j \sqrt{2g \frac{p_j - p_O}{\rho_j}}$$

where A_j is the physical area of the orifice. Measured values of the coefficient of discharge are presented in table I.

REFERENCES

1. Cox, H. Roxbee: British Aircraft Gas Turbines. Jour. Aero. Sci., vol. XIII, no. 2, Feb. 1946, pp. 53-83; discussion, pp. 83-87.

2. Chelko, Louis J.: Penetration of Liquid Jets Into a High-Velocity Air Stream. NACA RM E50F21, 1950.

3. Callaghan, Edmund E., and Ruggeri, Robert S.: A General Correlation of Temperature Profiles Downstream of a Heated-Air Jet Directed Perpendicularly to an Air Stream. NACA TN 2466, 1951.

4. Anon.: Tables of Thermodynamic Properties of Ammonia. Bur. Standards Cir. No. 142, Dept. Commerce, 1945.

TABLE I - AMMONIA INJECTION DATA

Ammonia jet velocity, V_j, ft/sec	Air velocity, V_0, ft/sec	Ammonia density, ρ_j, lb/cu ft	Air density, ρ_0, lb/cu ft	Ammonia temperature, T_j, °R	Air temperature, T_0, °R	Mixing distance, S, in.	Velocity ratio, $\frac{V_j}{V_0}$	Density ratio, $\frac{\rho_j}{\rho_0}$	Temperature ratio, $\frac{T_j}{T_0}$	Mixing distance parameter, $\frac{S}{\sqrt{CD_j}}$	$\sqrt{C}$	Penetration parameter, $\frac{y_1}{\sqrt{CD_j}}$	$\frac{y_1-y_2}{\sqrt{CD_j}}$	$\frac{\Delta T_m}{T_0-T_j}$	y_3, in.	y_4, in.	$\frac{x_1}{D_j}$	D_j, in.
114	112	41.2	0.0548	464	543	14	1.029	761	0.654	574	0.841	570	481	0.950	10.8	10.4	196	0.029
117	183	41.1	.0544	465	545		.634	756	.853	567	.852	418	377	.862	8.1	7.2	183	
116	227	41.2	.0543	462	544		.509	760	.849	578	.835	334	334	.805	6.0	5.3	197	
115	324	41.2	.0542	464	543		.354	759	.854	573	.843	245	262	.181	3.7	3.1	172	
59.6	327	40.9	.0541	470	543		.274	757	.866	616	.794	216	224	----	3.6	1.7	152	
105	326	41.0	.0541	468	543		.321	759	.862	589	.820	240	261	.440	3.1	2.7	162	
159	327	41.4	.0541	459	543		.486	766	.845	615	.795	307	329	.512	4.7	3.7	186	
114	146	42.0	.0699	448	543		.792	800	.821	592	.815	488	444	.849	8.5	7.8	196	
113	178	42.0	.0695	444	543		.634	805	.818	590	.819	407	387	.857	7.0	6.3	168	
113	253	42.0	.0698	444	543		.449	803	.818	594	.813	268	276	.598	4.6	3.9	162	
62.8	251	41.9	.0698	443	543		.251	800	.816	640	.755	186	210	.380	2.6	2.0	155	
96.6	265	41.9	.0699	443	542		.360	799	.817	592	.816	268	292	.404	3.5	2.4	165	
123	255	42.0	.0699	444	542		.484	802	.819	590	.819	282	303	.520	4.5	3.9	165	
162	254	42.1	.0700	442	541		.637	802	.817	624	.773	344	330	.636	5.0	4.3	167	
184	254	42.0	.0701	444	541		.728	800	.821	616	.783	347	330	.586	5.2	4.3	168	
208	254	42.0	.0701	445	541		.816	799	.823	602	.802	344	331	.677	5.0	4.7	179	
96.1	210	42.4	.0284	436	551	14	.459	1492	.791	584	.827	462	383	.939	8.7	6.3	238	0.029
96.0	192	42.5	.0398	434	551		.500	1068	.788	586	.809	390	332	.701	7.7	7.0	194	
96.3	197	42.4	.0483	435	552		.498	880	.788	592	.815	347	271	.462	6.3	5.6	169	
97.4	198	42.4	.0581	436	552		.492	730	.790	587	.822	325	283	.405	5.3	4.6	172	
97.7	196	42.3	.0676	439	552		.496	626	.795	587	.822	289	261	.345	4.8	3.9	165	
89.8	184	42.0	.0240	444	661		.488	1752	.672	598	.808	440	410	.600	10.0	9.5	152	
91.7	197	42.0	.0300	445	662		.466	1400	.672	591	.816	385	309	.506	8.5	8.5	148	
92.3	197	42.0	.0398	444	666		.470	1056	.667	589	.819	337	286	.509	6.6	5.9	145	
92.2	197	42.0	.0490	445	661		.469	858	.673	590	.819	284	244	.315	5.5	4.5	134	
91.5	194	42.0	.0568	444	664		.471	740	.669	586	.824	289	272	.323	5.3	5.0	148	
96.5	306	41.2	.0480	463	552	14	.319	858	.839	628	.768	245	274	.483	3.9	2.9	152	0.029
78.0	295	41.2	.0494	462	665		.264	936	.695	630	.766	216	225	.246	2.9	2.5	134	
92.4	293	41.2	.0493	464	711		.315	836	.653	672	.718	209	208	.182	2.8	2.1	124	
91.6	290	41.2	.0496	462	765		.317	831	.604	696	.695	176	183	.152	2.7	2.3	114	
89.0	291	41.3	.0509	438	549		.306	852	.798	577	.836	250	264	.459	3.3	2.6	176	
89.5	291	41.9	.0502	447	549		.306	855	.814	594	.813	260	284	.451	3.0	2.1	176	
90.3	294	41.3	.0492	460	553		.308	840	.832	600	.804	251	262	.518	3.1	2.7	166	
90.8	295	41.0	.0489	458	552		.308	839	.848	612	.789	244	262	.607	3.4	2.7	179	
92.1	294	41.2	.0502	464	610		.313	1362	.761	611	.790	306	310	.603	4.8	4.0	148	
91.4	292	41.2	.0501	464	660		.313	1367	.703	624	.774	279	287	.403	4.8	3.8	155	
90.8	292	41.2	.0300	464	712		.311	1373	.652	643	.751	306	330	----	2.6	2.3	145	
90.9	303	41.2	.0296	464	770		.230	1392	.605	602	.802	233	244	----	2.6	1.1	---	
88.2	311	42.5	.0307	433	543		.284	1387	.797	599	.806	310	321	.90	5.3	4.2	188	
86.9	306	42.0	.0307	445	543		.284	1370	.820	596	.810	311	319	.918	5.4	4.0	193	
89.7	306	41.7	.0305	452	543		.293	1369	.832	617	.782	320	326	.98	5.2	3.8	190	
90.3	298	41.2	.0304	463	543		.303	1358	.853	629	.767	317	332	.95	5.9	3.9	186	
126	198	41.9	.0492	447	545	4	.634	852	.820	172	.802	249	185	1.89	4.7	2.6	117	0.029
126	202	42.0	.0488	444	547	8	.621	862	.812	344	.802	309	219	1.60	5.5	4.7	166	
125	198	42.2	.0493	441	548	24	.651	856	.804	1031	.802	520	563	.324	8.5	6.8	221	
126	321	41.9	.0492	447	544	4	.391	853	.822	172	.802	157	186	1.91	2.9	2.0	103	
125	322	42.1	.0492	443	544	8	.390	856	.814	344	.802	218	153	1.11	2.7	2.3	134	
126	320	42.0	.0493	444	544	24	.394	853	.816	1031	.802	322	378	.290	3.3	2.0	210	
124	201	42.0	.0686	444	546	4	.634	613	.813	172	.802	203	129	1.73	3.8	2.1	107	
123	200	42.1	.0687	442	546	8	.639	613	.810	344	.802	258	208	1.54	4.9	3.6	152	
128	200	41.9	.0684	447	548	24	.638	615	.819	1031	.802	422	442	.263	5.9	4.0	214	
126	148	42.1	.0571	443	535	14	.863	757	.628	347	.761	333	278	1.96	10.1	9.0	179	0.053
126	180	42.1	.0574	442	535		.701	734	.626	347	.762	280	236	1.70	7.2	6.8	166	
125	232	42.1	.0571	443	535		.538	738	.628	346	.764	198	170	1.25	6.7	4.9	147	
126	343	42.1	.0572	443	534		.369	736	.630	347	.762	148	144	1.10	4.1	3.7	121	
75.7	333	42.3	.0572	439	534		.227	739	.622	347	.761	122	134	.863	3.0	2.0	108	
39.6	333	42.2	.0573	441	534		.299	736	.626	344	.767	140	135	1.08	3.7	2.6	111	
121	333	42.2	.0573	441	534		.364	736	.626	320	.827	152	128	1.15	4.5	3.9	121	
157	333	42.1	.0573	442	534		.472	736	.628	347	.762	161	161	1.03	4.8	3.8	134	
112	133	42.0	.0558	445	550	14	.839	753	.809	1174	.883	957	963	.305	9.7	9.7	211	0.018
112	174	41.9	.0560	442	549		.644	748	.805	1158	.872	661	728	.318	8.1	4.9	216	
112	216	42.0	.0560	446	549		.512	750	.812	1172	.864	643	610	.349	4.6	3.9	216	
111	323	42.2	.0567	441	545		.345	744	.809	1162	.869	352	390	.280	2.5	1.7	172	
114	329	42.0	.0562	445	547		.347	748	.814	1168	.866	392	---	.234	2.7	1.9	---	
161	329	42.0	.0562	448	546		.489	746	.817	1069	.734	469	481	.330	5.2	2.4	216	
212	327	42.0	.0566	445	545		.651	743	.816	1010	.770	440	425	.300	4.2	2.5	216	
244	326	42.0	.0565	446	546		.753	743	.817	936	.781	470	469	.320	4.4	2.8	218	

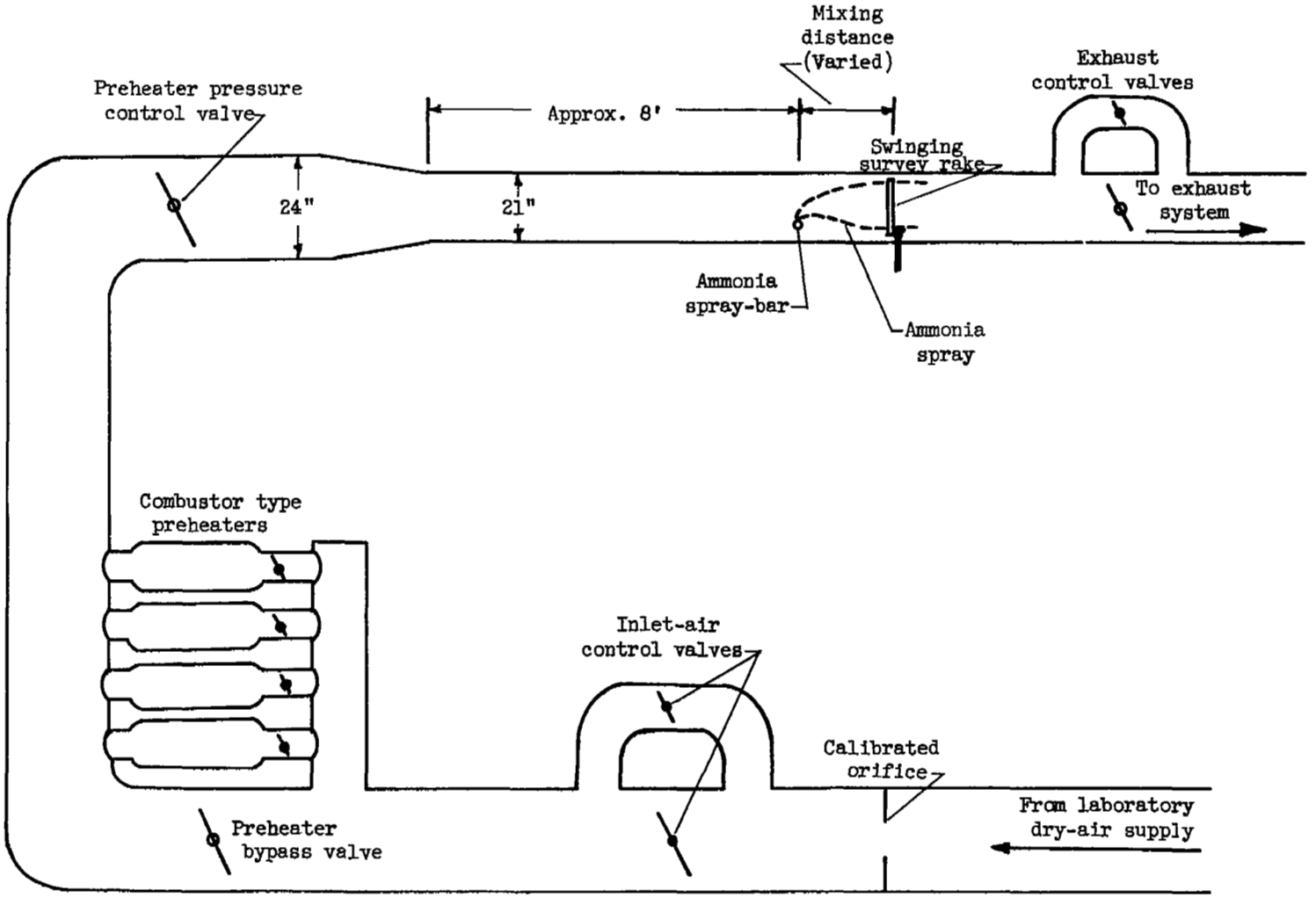

Figure 1. - Schematic diagram of air system.

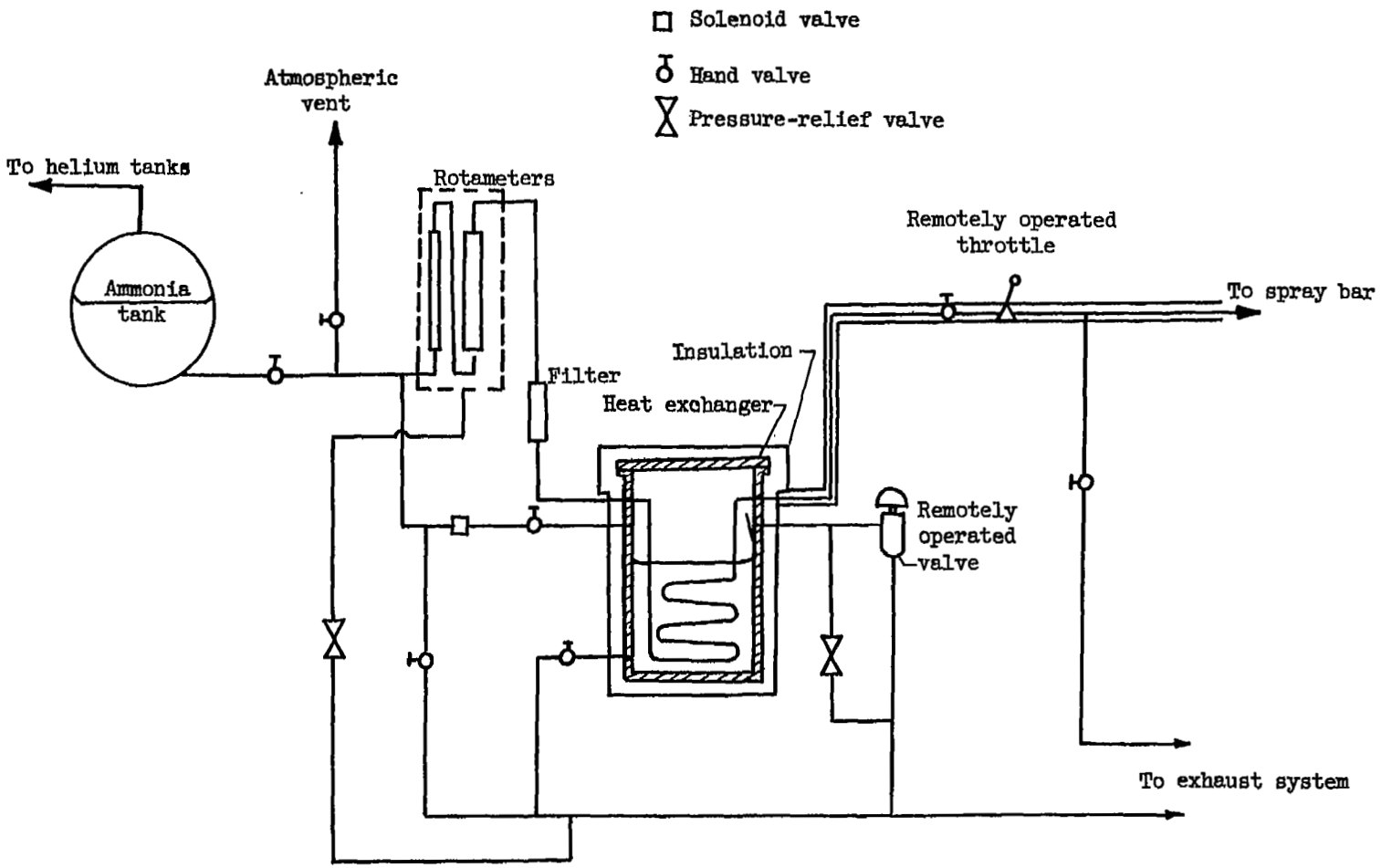

Figure 2. - Schematic diagram of ammonia system.

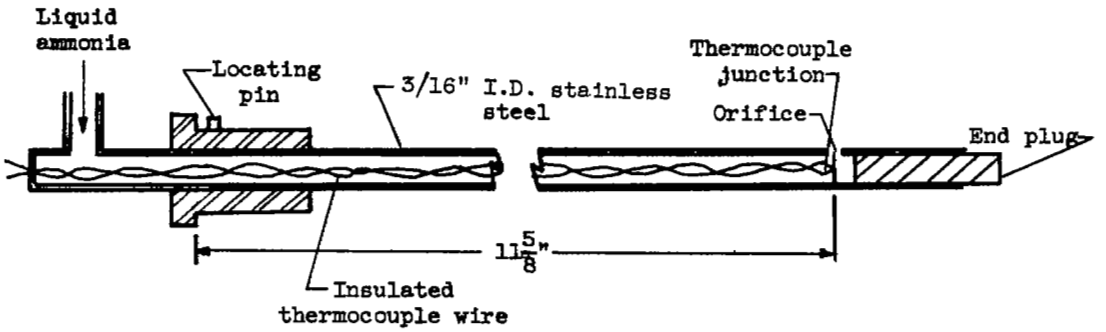

Figure 3. - Schematic diagram of ammonia spray-bar.

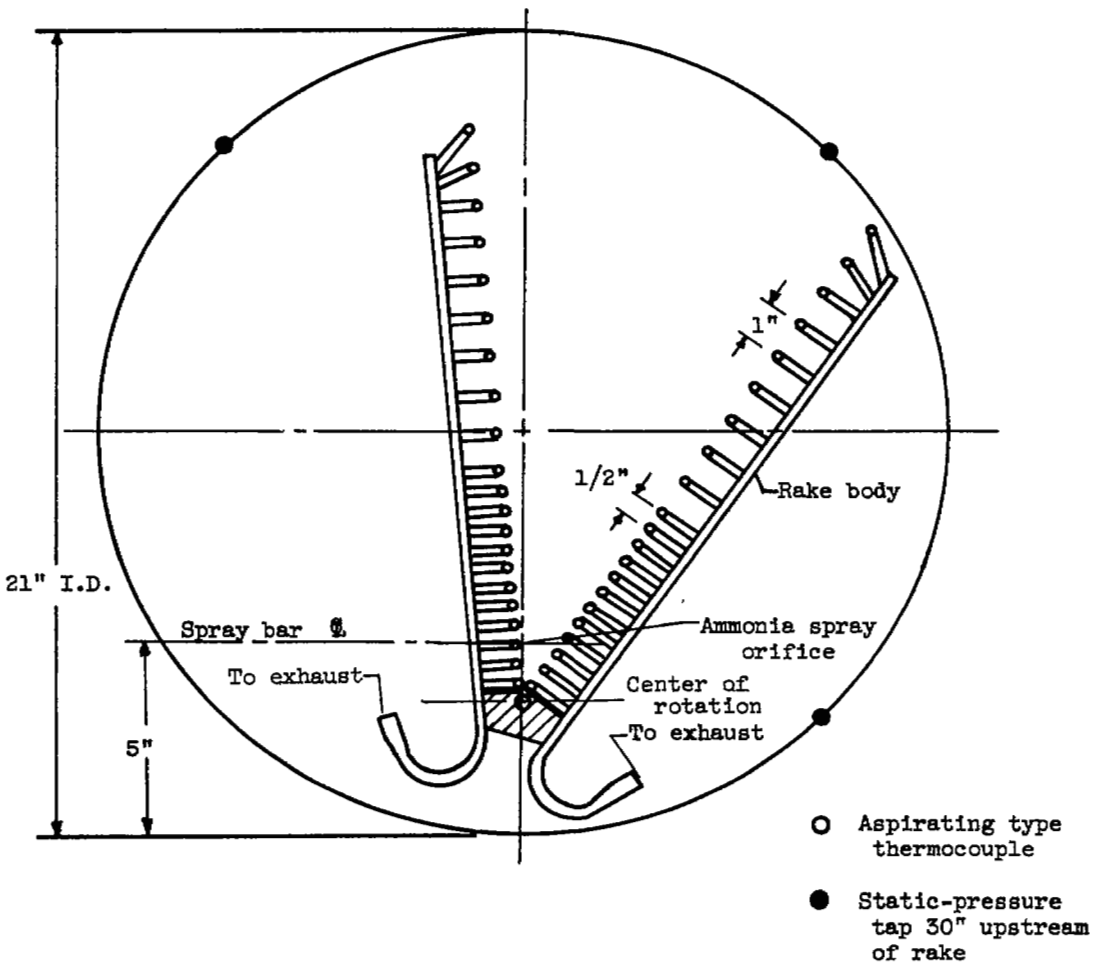

Figure 4. - Schematic diagram of swinging temperature-survey rake.

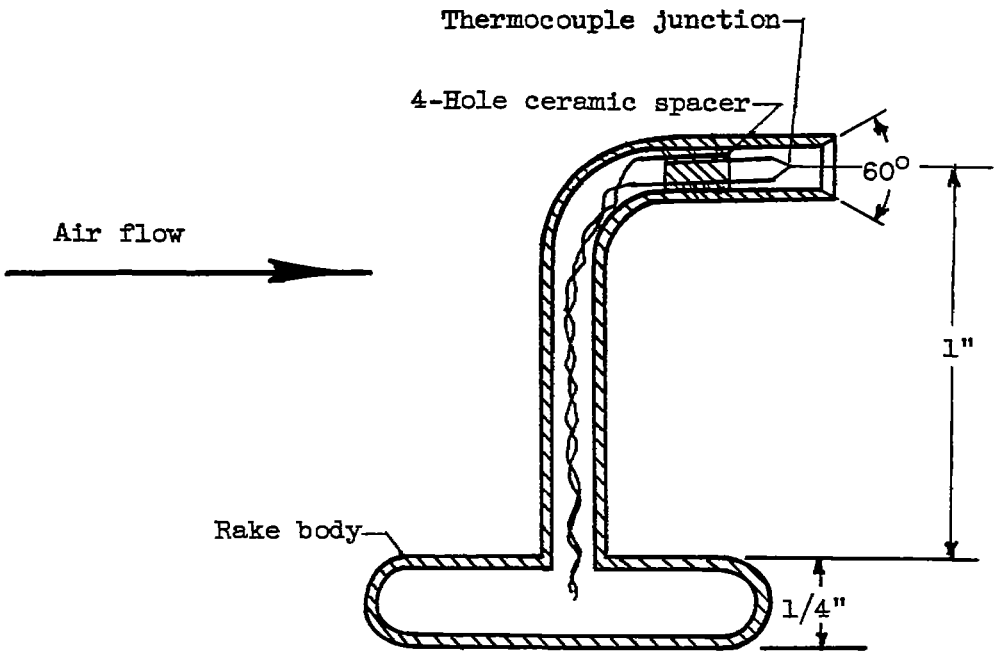

Figure 5. - Schematic diagram of aspirating-type thermocouple used on swinging temperature survey rake.

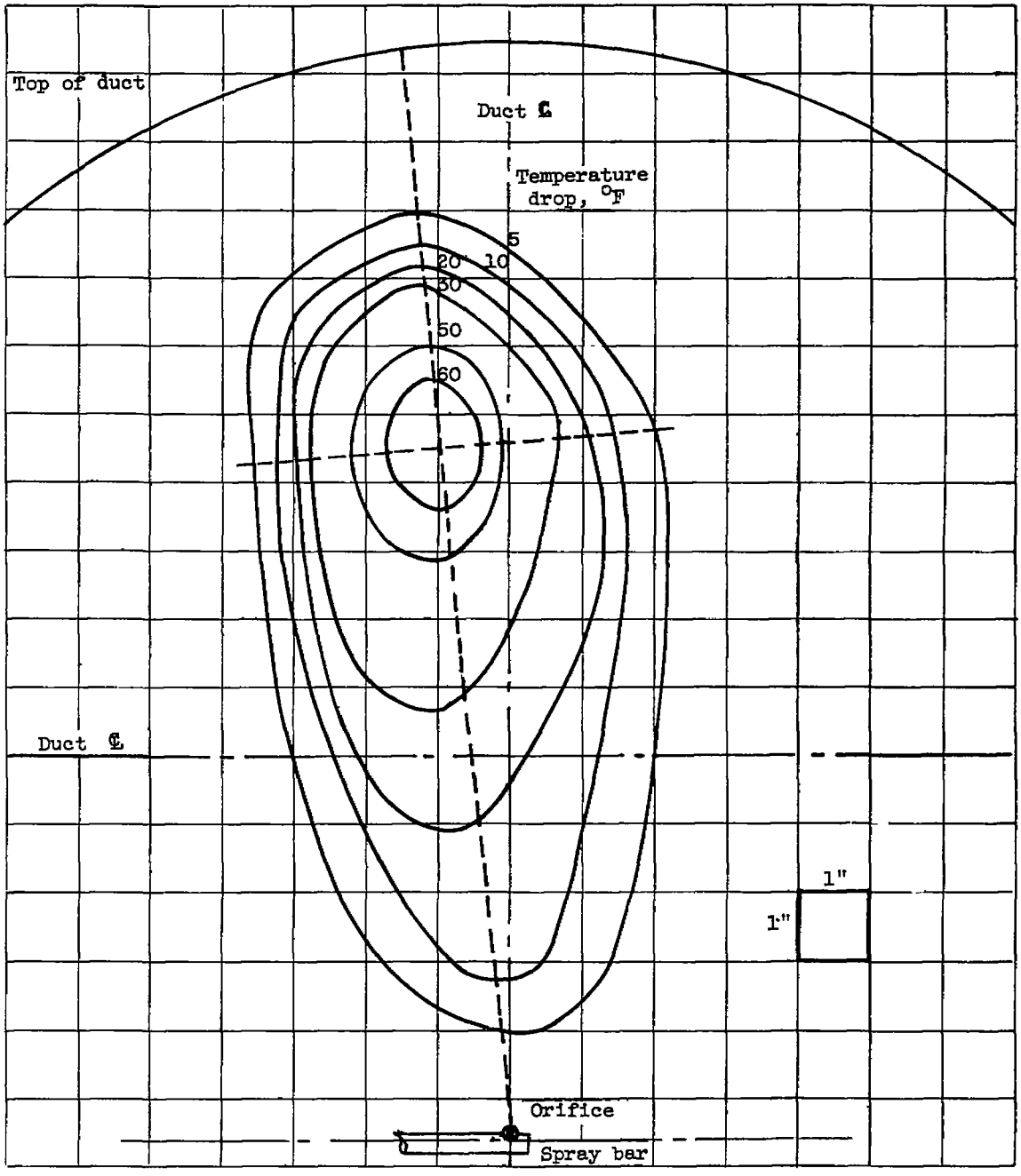

(a) Air velocity, 112 feet per second.

Figure 6. - Typical isothermal contour maps determined for range of air velocities. Ammonia velocity, 82.7 feet per second; air density, 0.054 pound per cubic foot; ammonia dentisy, 41.2 pounds per cubic foot; air temperature, 544° R; ammonia temperature, 464° R; mixing distance, 14 inches; and orifice diameter, 0.029 inch.

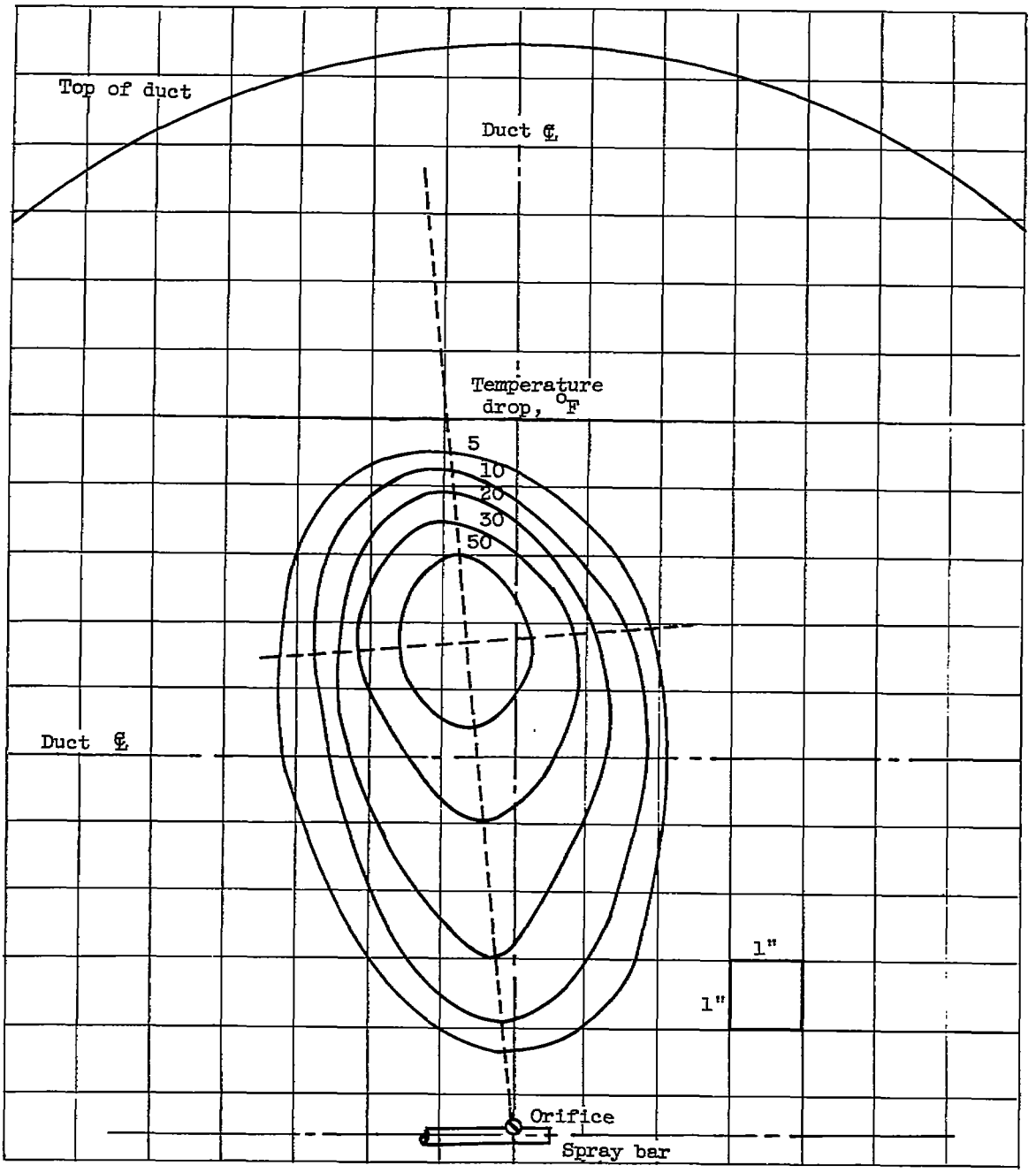

(b) Air velocity, 183 feet per second.

Figure 6. - Continued. Typical isothermal contour maps determined for range of air velocities. Ammonia velocity, 82.7 feet per second; air density, 0.054 pound per cubic foot; ammonia density, 41.2 pounds per cubic foot; air temperature, 544° R; ammonia temperature, 464° R; mixing distance, 14 inches; and orifice diameter, 0.029 inch.

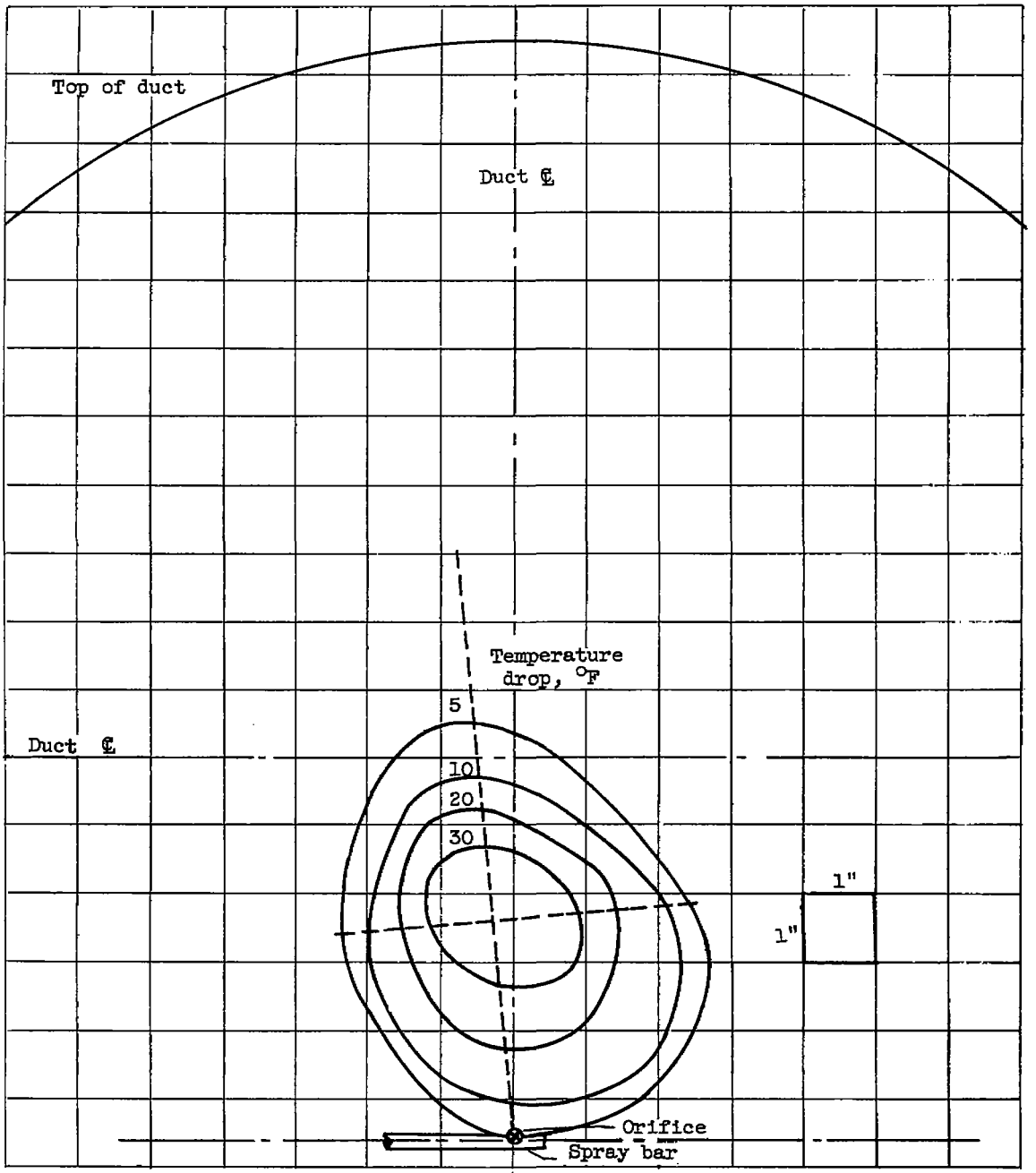

(c) Air velocity, 324 feet per second.

Figure 6. - Concluded. Typical isothermal contour maps determined for range of air velocities. Ammonia velocity, 82.7 feet per second; air density, 0.054 pound per cubic foot; ammonia density, 41.2 pounds per cubic foot; air temperature, 544° R; ammonia temperature, 464° R; mixing distance, 14 inches; and orifice diameter, 0.029 inch.

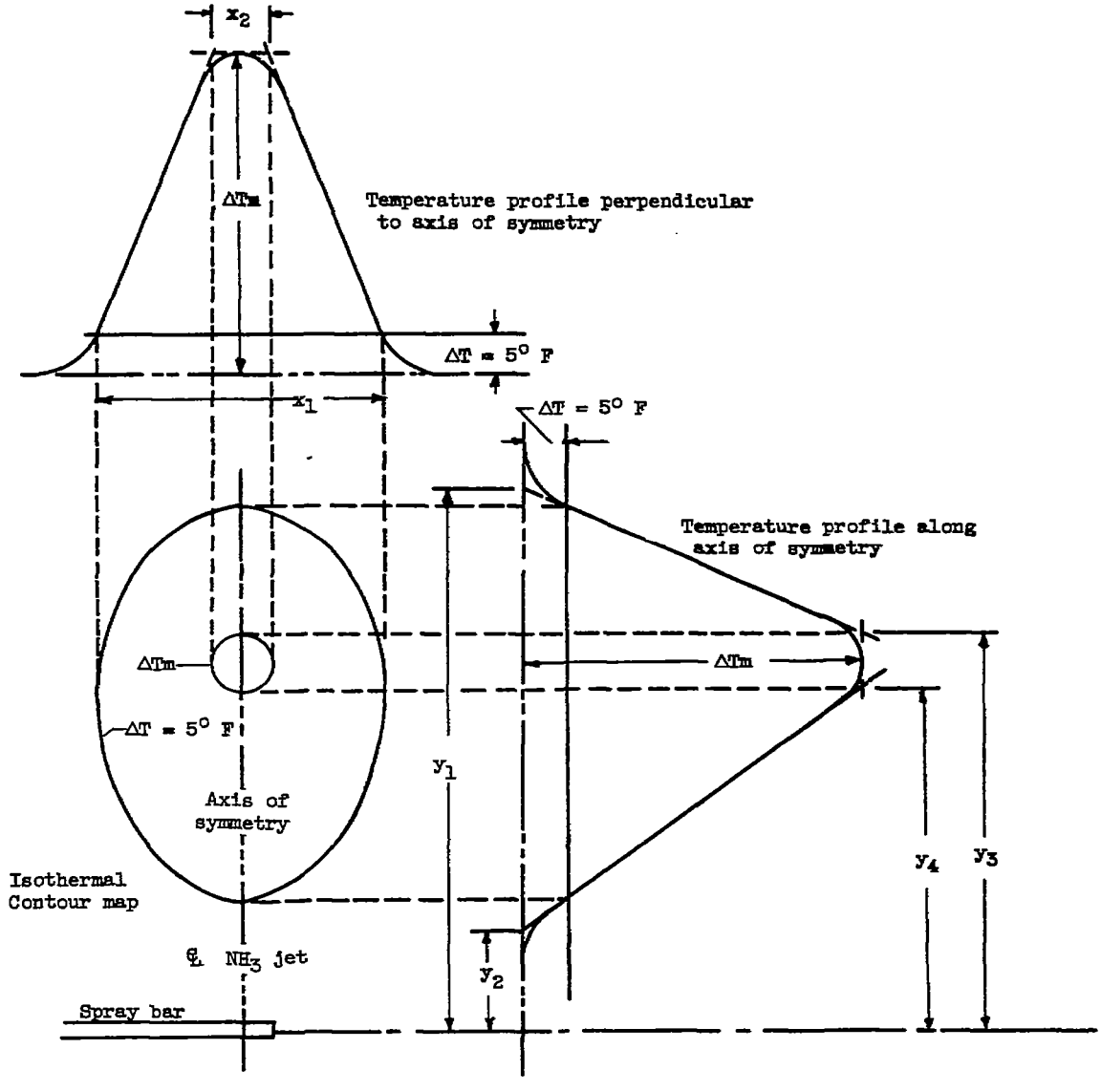

Figure 7. - Dimensions selected for correlation of isothermal contour map formed by injection of liquid ammonia normal to air stream.

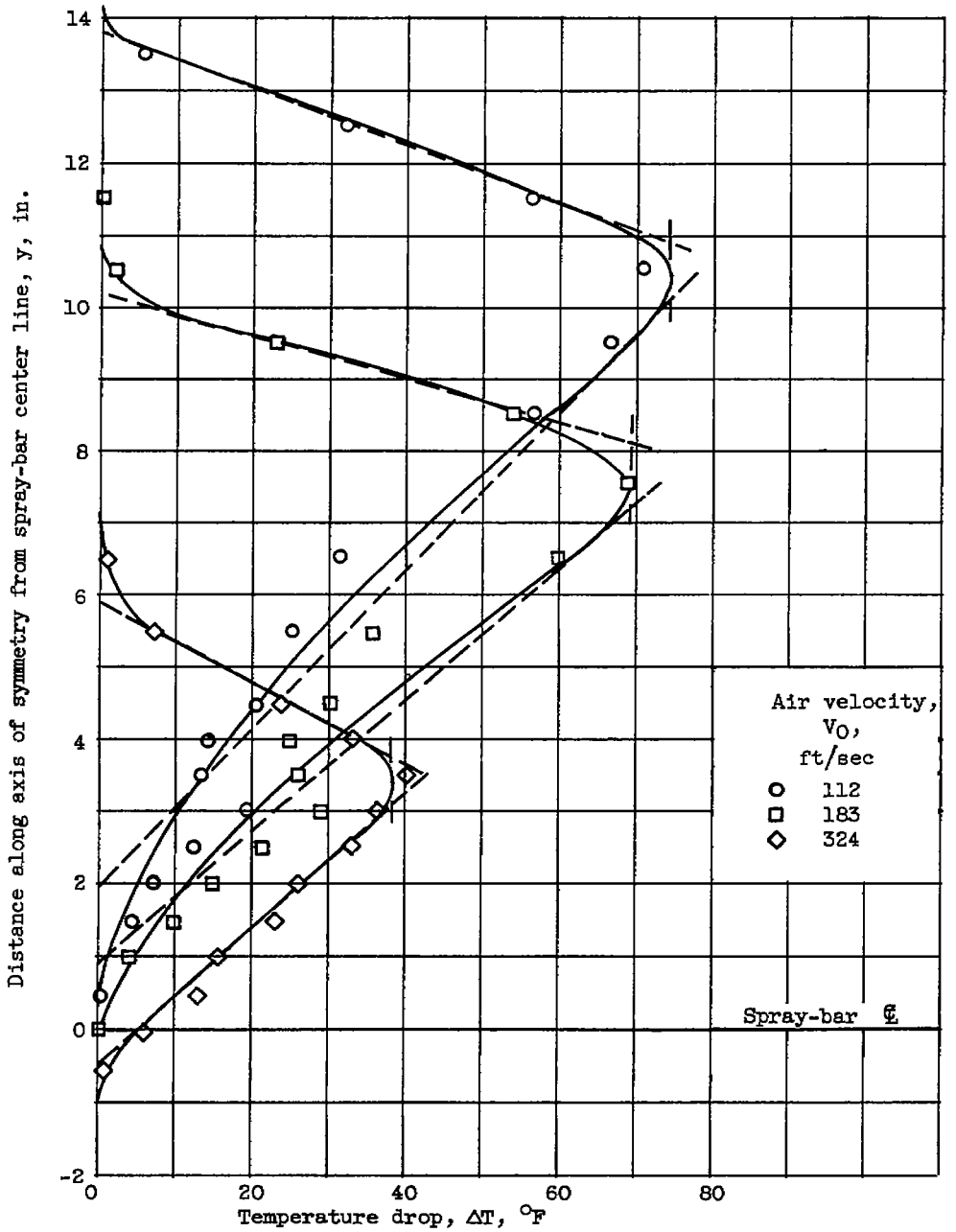

Figure 8. - Typical temperature profiles along axis of symmetry together with respective bounding tangents for range of air velocities. Ammonia velocity 82.7 feet per second; air density, 0.054 pound per cubic foot; ammonia density, 41.2 pound per cubic foot; air temperature, of 544° R; ammonia temperature, 464° R; mixing distance, 14 inches; and orifice diameter, 0.029 inch.

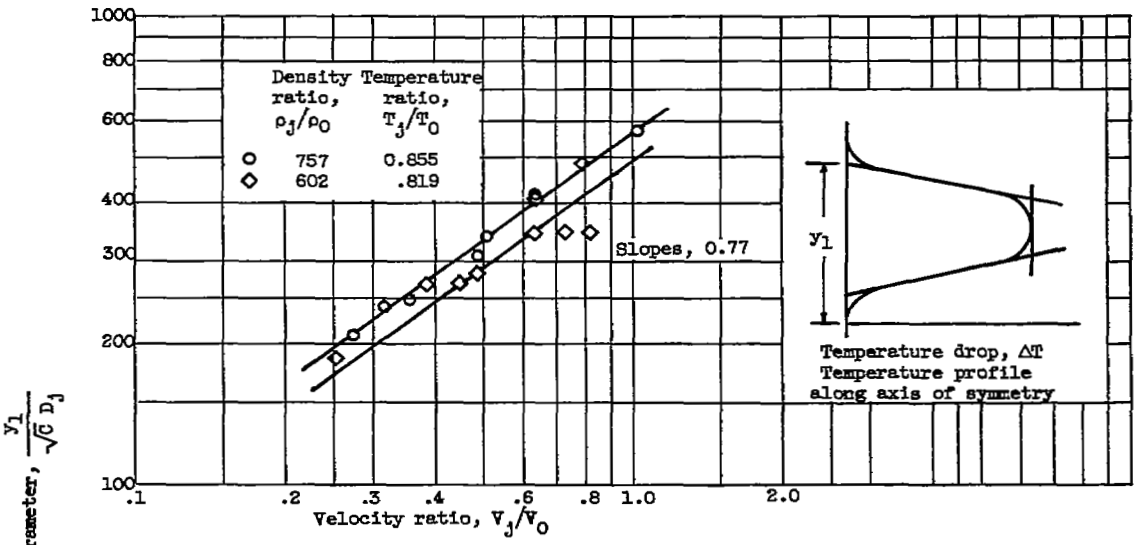

(a) Effect of velocity ratio on penetration parameter for two density ratios. Orifice diameter, 0.029 inch; mixing distance, 14 inches.

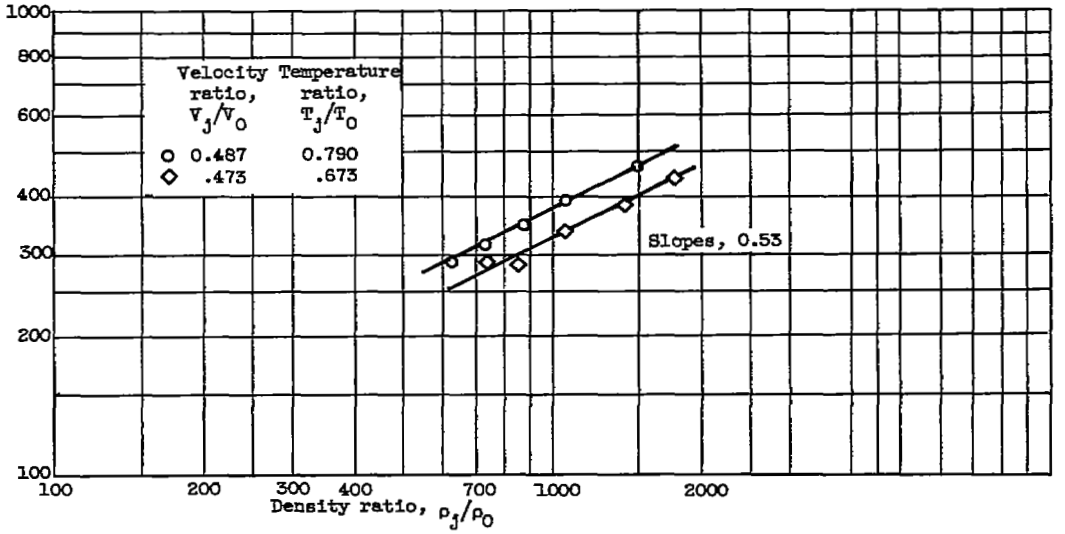

(b) Effect of density ratio on penetration parameter for two temperature ratios. Orifice diameter, 0.029 inch; mixing distance, 14 inches.

Figure 9. - Correlation of boundary dimension y_1.

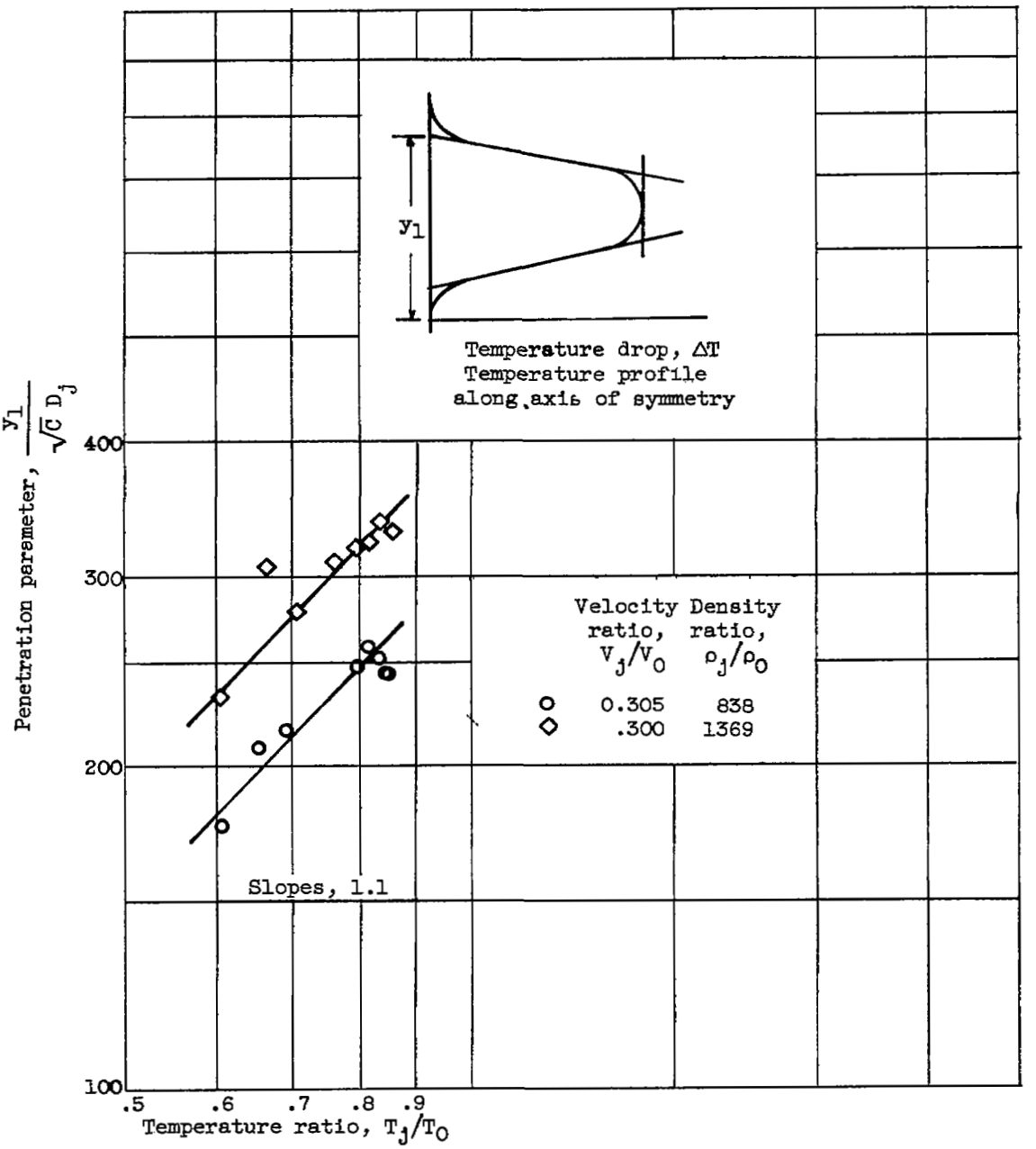

(c) Effect of temperature ratio on penetration parameter for two density ratios. Orifice diameter, 0.029 inch; mixing distance, 14 inches.

Figure 9. - Continued. Correlation of boundary dimension y_1.

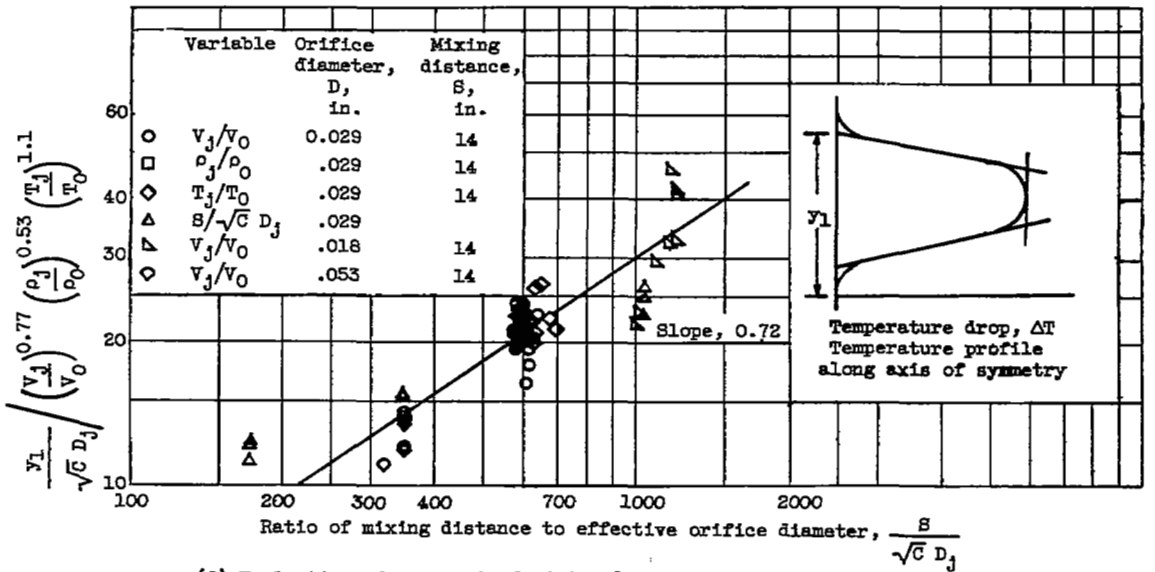

(d) Evaluation of exponent of mixing distance to effective diameter ratio.

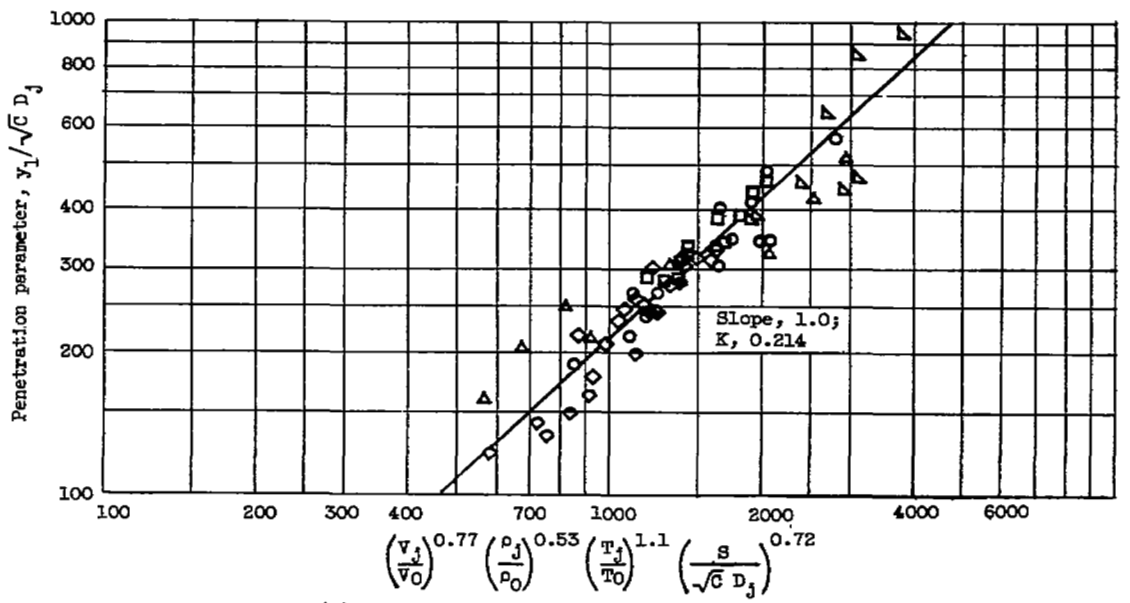

(e) Final correlation of penetration parameter

Figure 9. - Concluded. Correlation of boundary dimension y_1.

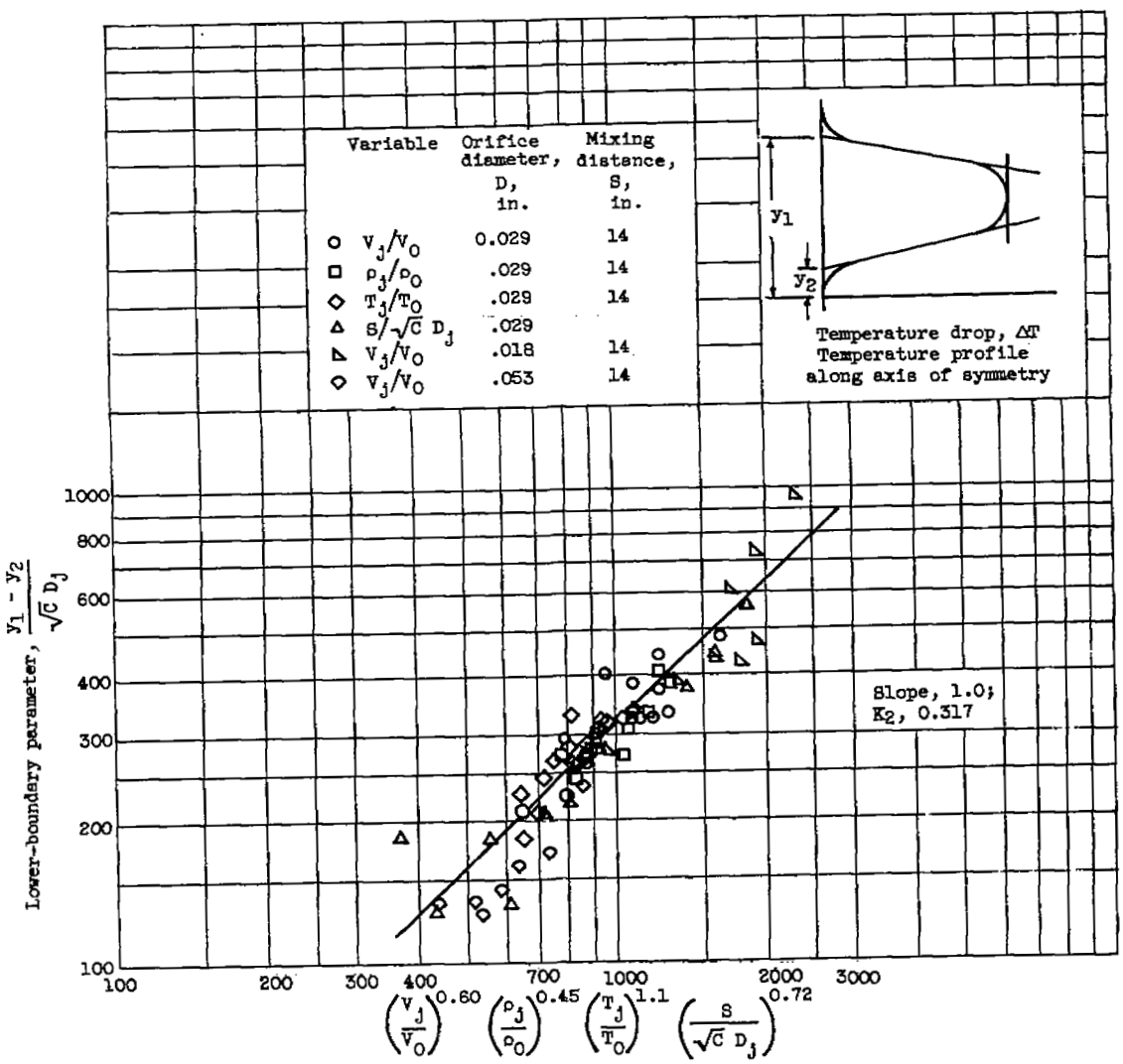

Figure 10. - Correlation of lower-boundary defining parameter of temperature profile along axis of symmetry.

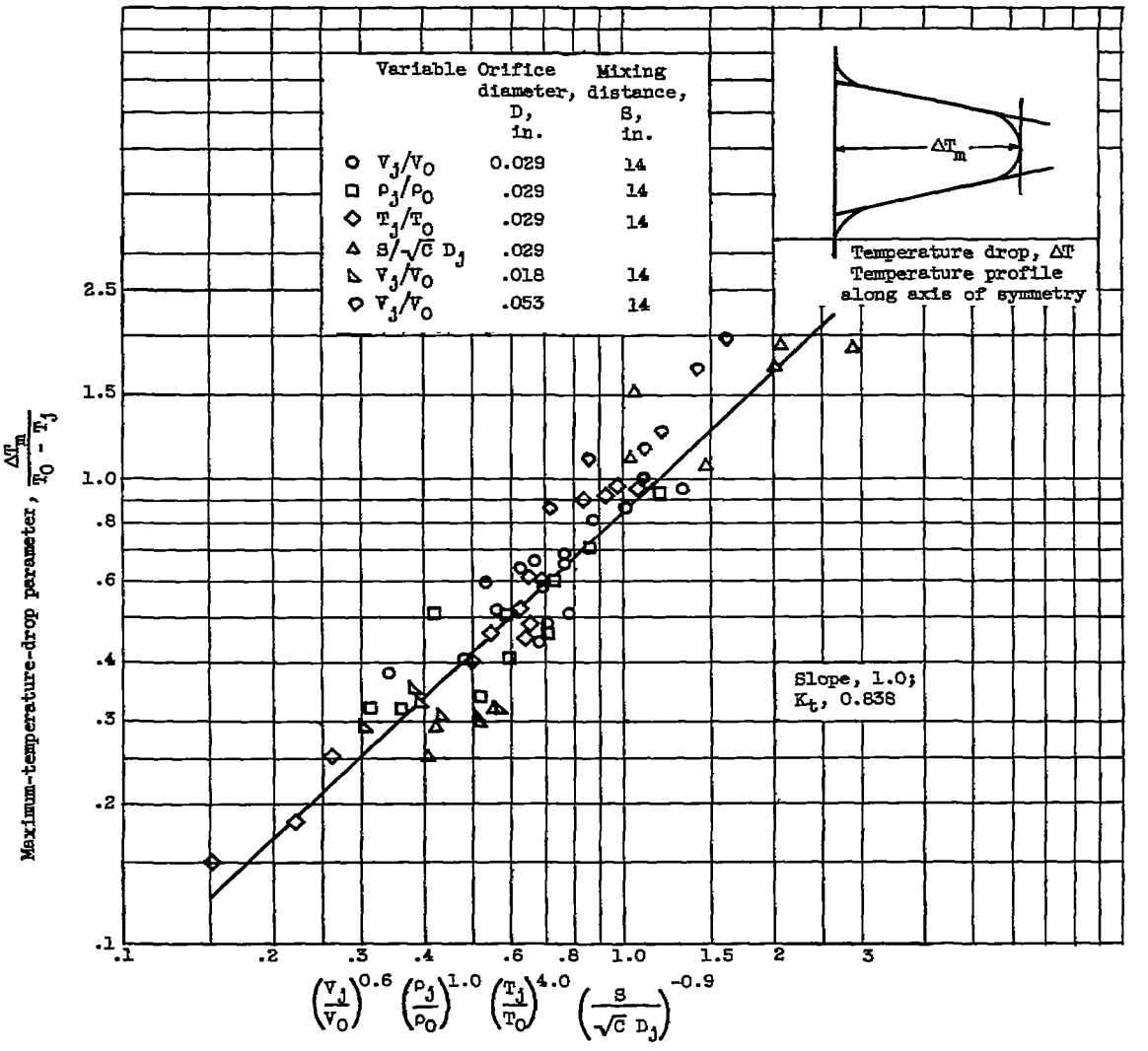

Figure 11. - Correlation of maximum-temperature-drop parameter.

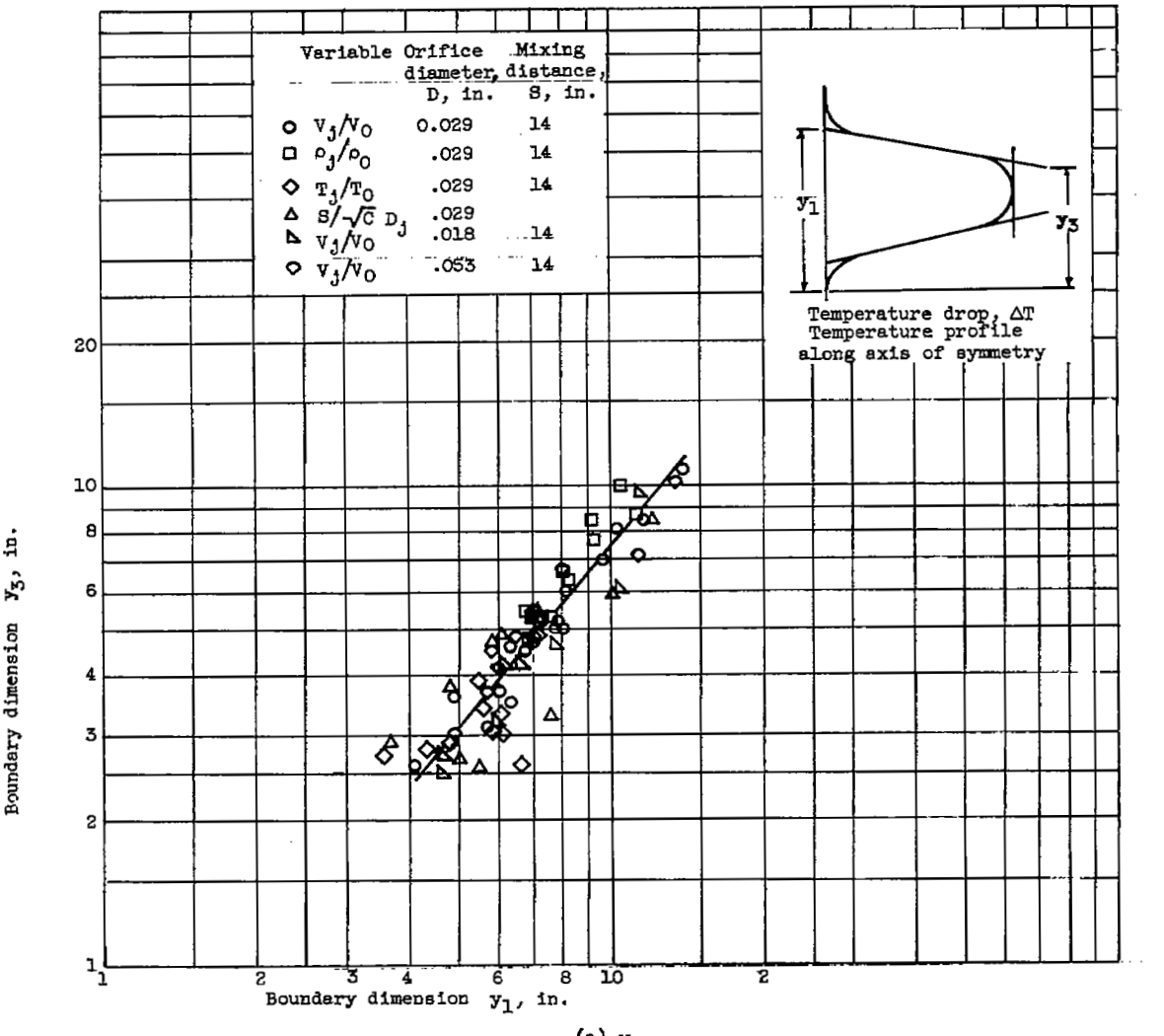

(a) y_3.

Figure 12. - Correlation of boundary dimensions in terms of boundary dimension y_1.

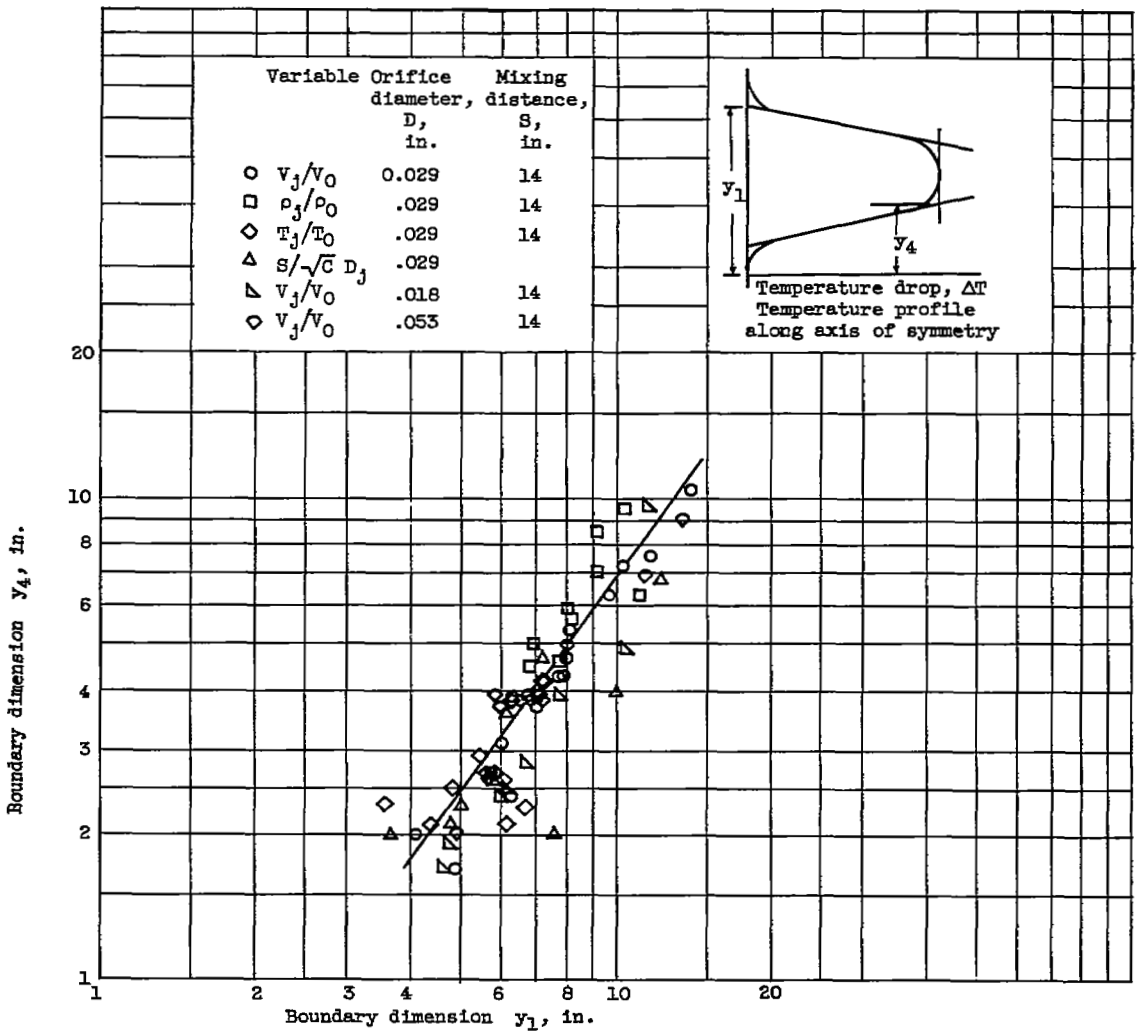

(b) y_4.

Figure 12. - Concluded. Correlation of boundary dimensions in terms of boundary dimension y_1.

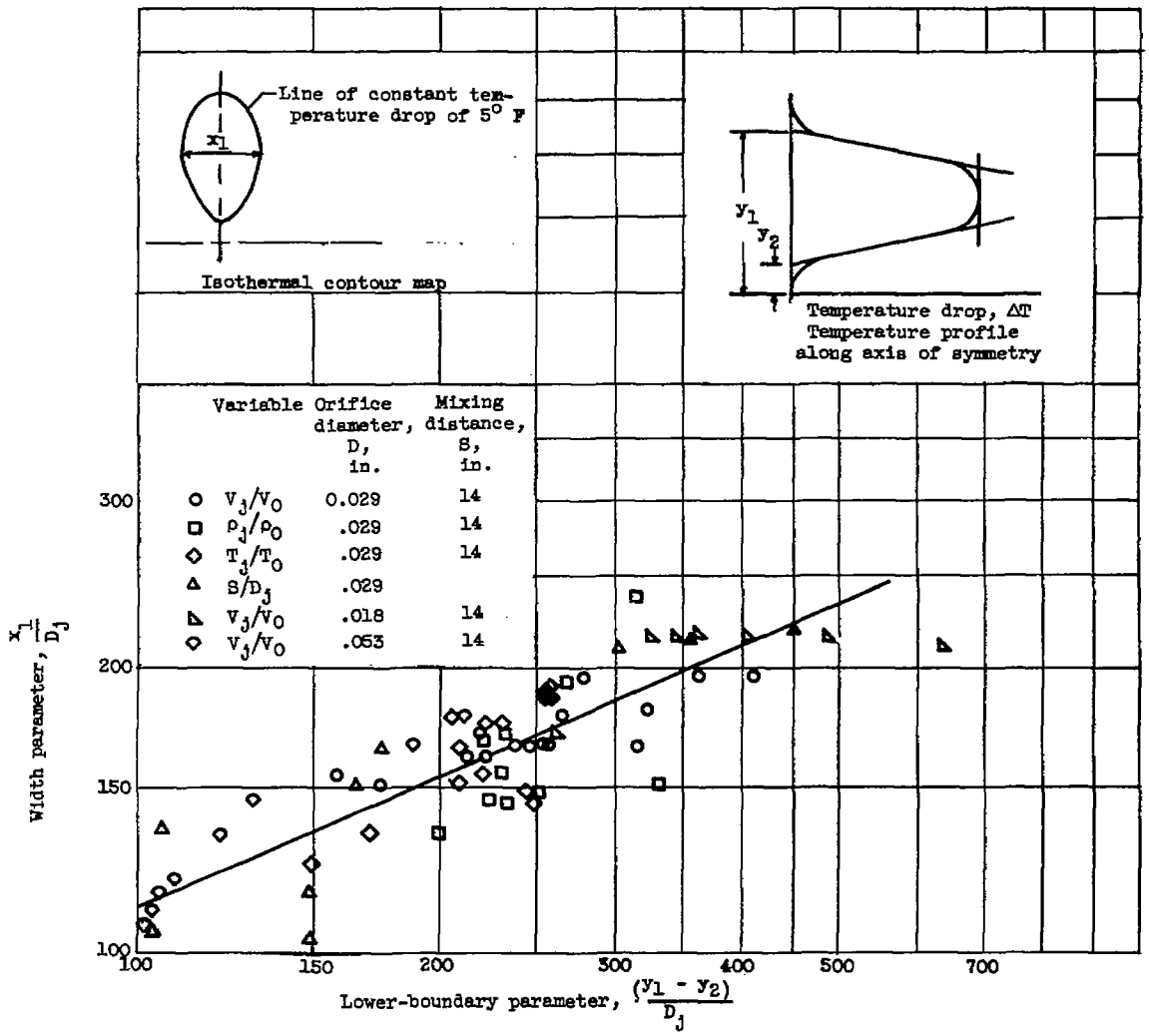

Figure 13. - Correlation of width parameter with lower-boundary parameter.

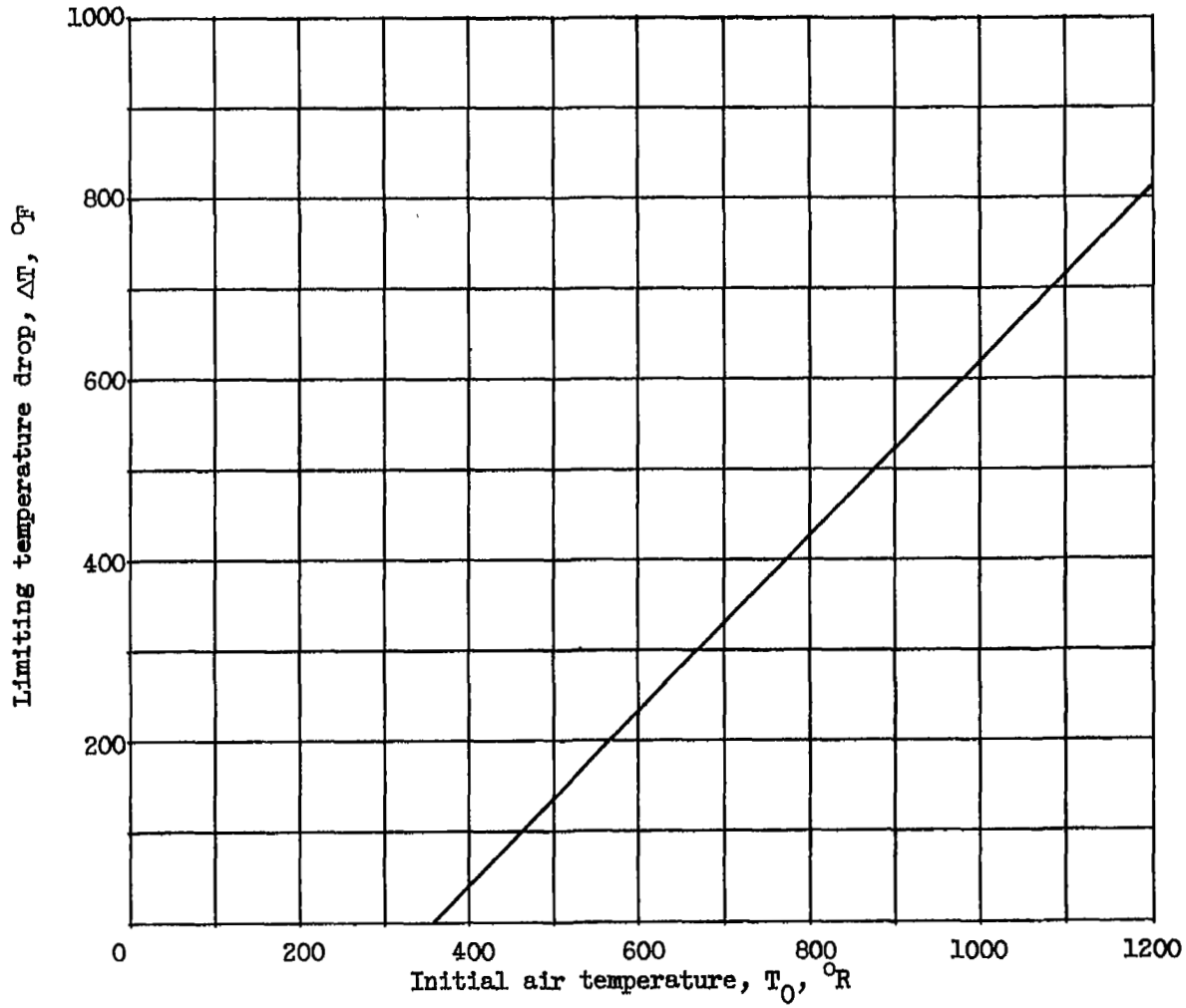

Figure 14. - Limiting temperature drop obtainable by saturating dry air with ammonia vapor. Constant-pressure process in which all cooling is accomplished by latent heat of vaporization of liquid ammonia is assumed.

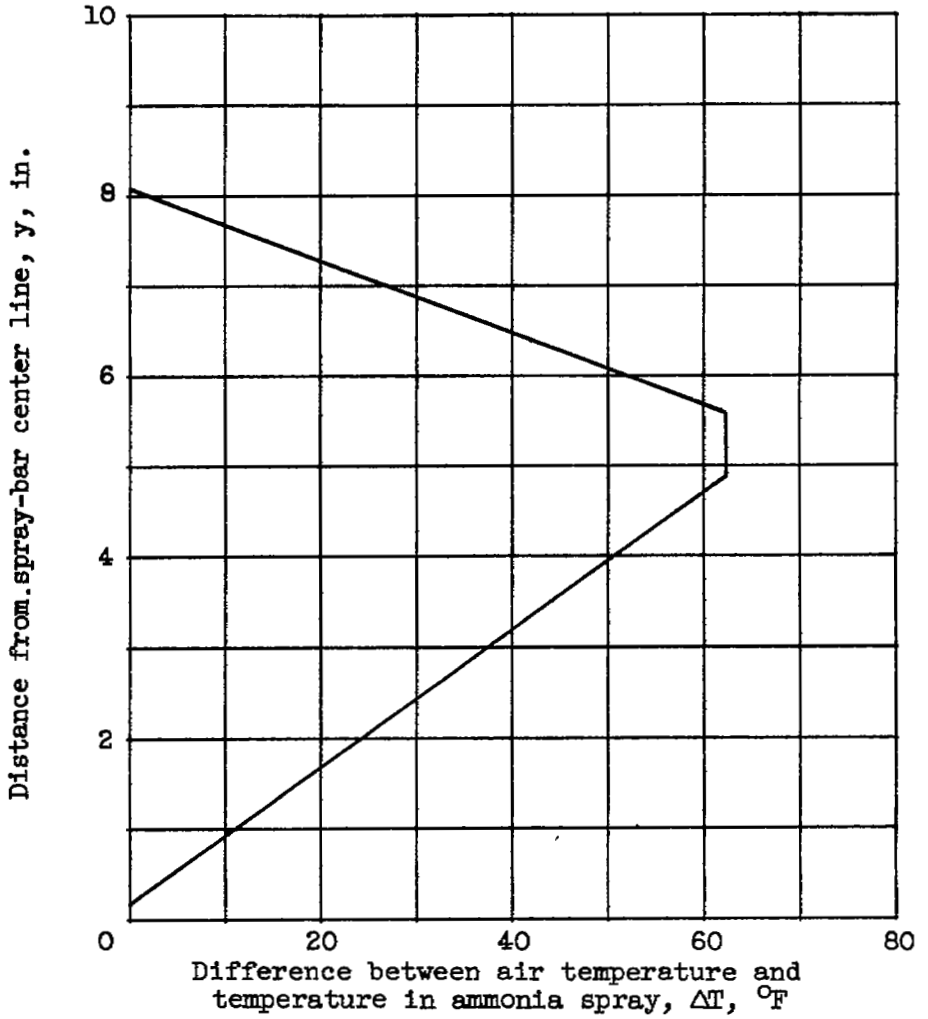

(a) Temperature profile along axis of symmetry constructed from correlation.

Figure 15. - Prediction of isothermal contour map for double-orifice injection system. Velocity ratio, 0.52; density ratio, 741; temperature ratio, 0.82; mixing distance to diameter ratio, 560.

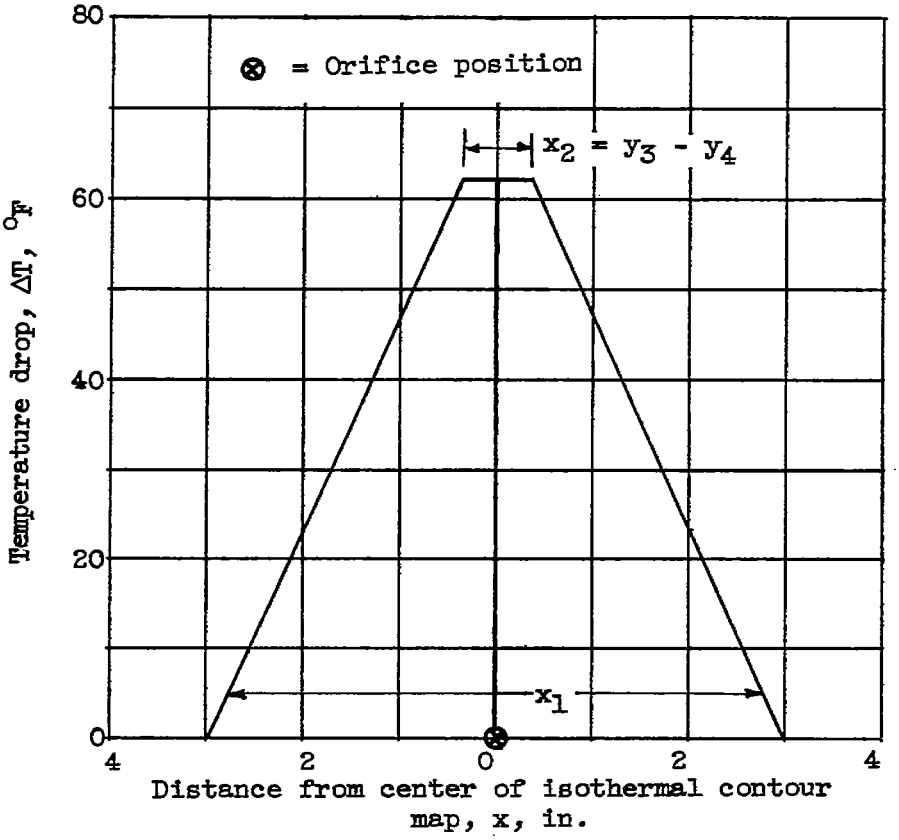

(b) Temperature profile perpendicular to axis of symmetry constructed from correlation.

Figure 15. - Continued. Prediction of isothermal contour map for double-orifice injection system. Velocity ratio, 0.52; density ratio, 741; temperature ratio, 0.82; mixing distance to diameter ratio, 560.

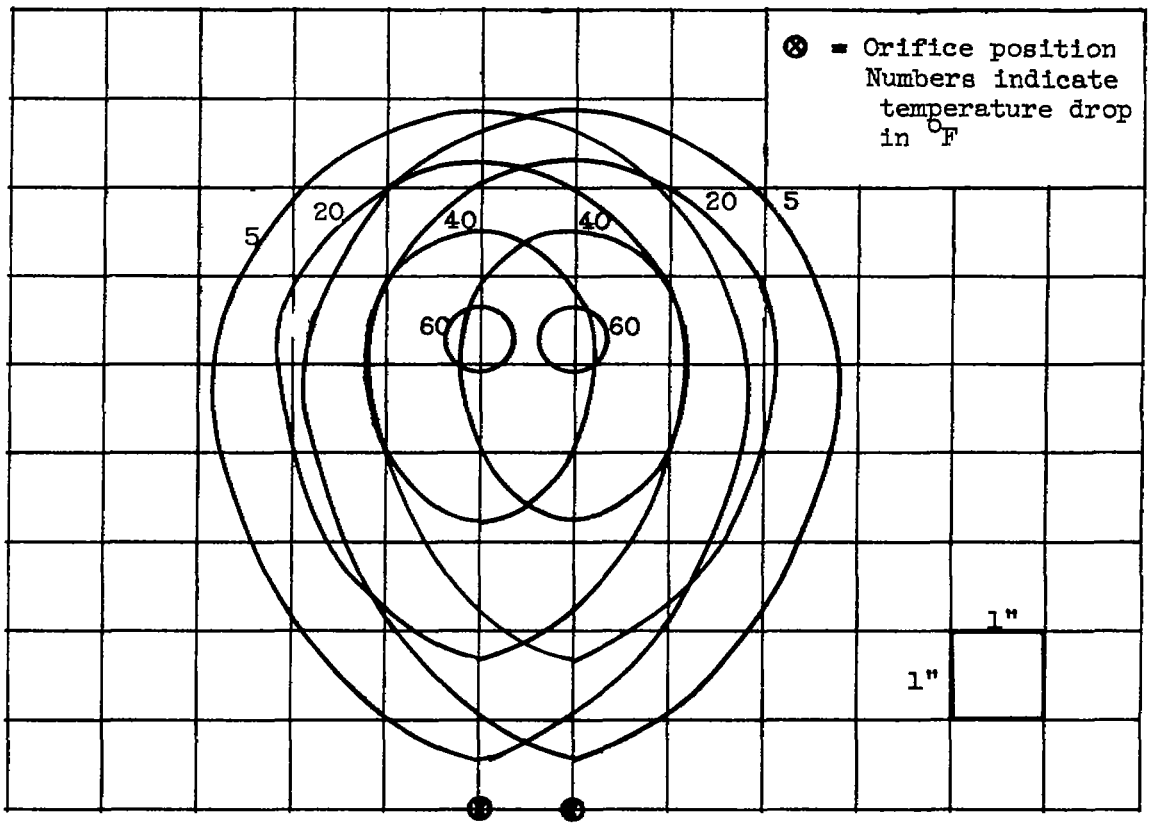

(c) Two predicted single-orifice isothermal contour maps superimposed to represent double-orifice system.

Figure 15. - Continued. Prediction of isothermal contour map for double-orifice injection system. Velocity ratio, 0.52; density ratio, 741; temperature ratio, 0.82; mixing distance to diameter ratio, 560.

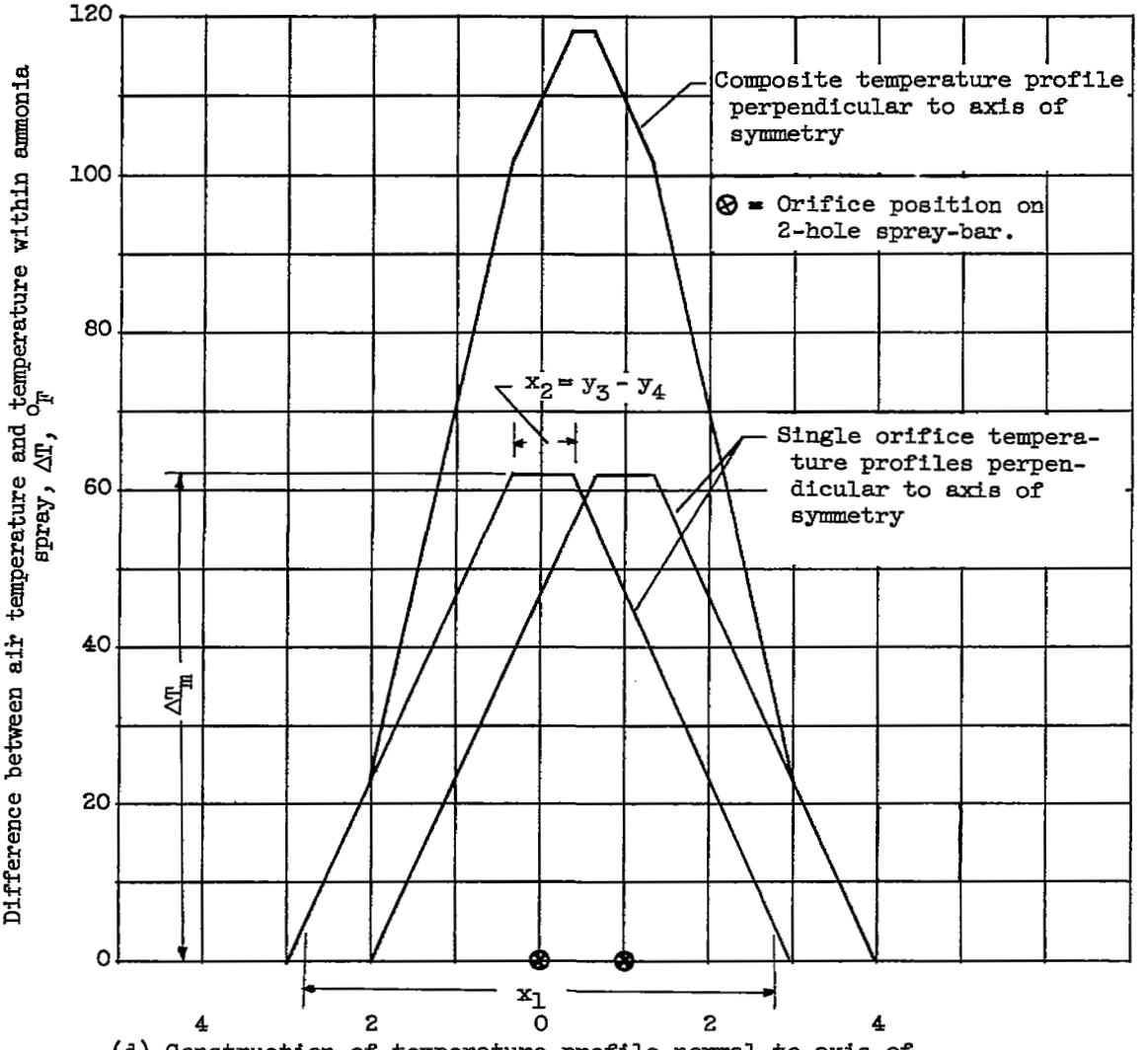

(d) Construction of temperature profile normal to axis of symmetry of double-orifice isothermal contour map.

Figure 15. - Continued. Prediction of isothermal contour map for double-orifice injection system. Velocity ratio, 0.52; density ratio, 741; temperature ratio, 0.82; mixing distance to diameter ratio, 560.

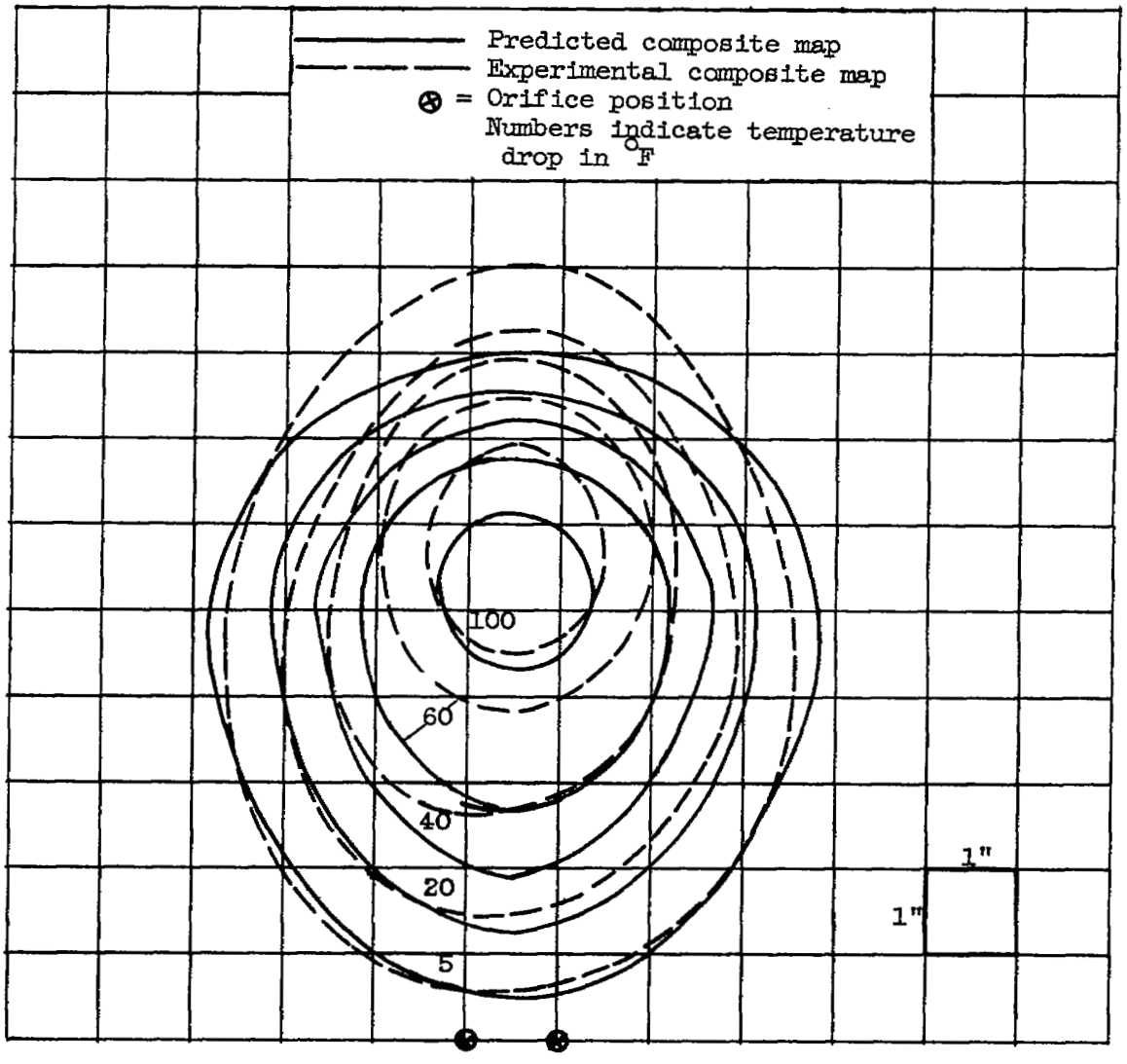

(e) Comparison of predicted and experimental isothermal contour maps double-orifice injection system.

Figure 15. - Concluded. Prediction of isothermal contour map for double-orifice injection system. Velocity ratio, 0.52; density ratio, 741; temperature ratio, 0.82; mixing distance to diameter ratio, 560.